Table 1 – Percentage of each cell population in liver during development.

	E11.5	E12.5	E14.5	E16.5
$EpCAM^+DLK1^+$/total cells (%)	8.4	3.6	1.9	0.3
$DLK1^+$/total cells (%)	18.0	10.4	8.1	3.9
$EpCAM^+DLK1^+$ cells (%)	46.7	34.4	23.5	6.7

as a ductal plate (Figs. 1A and 3D). These $EpCAM^+$ cells were negative for DLK1, as previously reported (Tanimizu et al., 2003).

To reveal the detailed expression profiles of EpCAM and DLK1 during liver development, we performed FCM of fetal liver cells at E11.5, E12.5, E14.5 and E16.5, because it allows more sensitive and quantitative detection than IHC. FCM revealed that approximately 20% of nucleated cells in E11.5 liver were $DLK1^+$ cells, about half of which expressed EpCAM (Fig. 4). Interestingly, the percentage of $EpCAM^+$ cells in the $DLK1^+$ cell population was rapidly reduced along with liver development (Table 1). Moreover, the expression level of EpCAM after E12.5 was very low compared with that of E11.5 liver. Downregulation of EpCAM in $DLK1^+$ cells by FCM was consistent with the results of IHC and RT-PCR in fetal liver from E11.5 to E17.5 (Figs. 1B and 3A–D). These results suggested that EpCAM is highly expressed at the onset of liver organogenesis, dramatically decreased along with hepatic differentiation, and then restricted to intrahepatic bile duct cells at a later stage.

2.4. *Colony formation capacity of $EpCAM^+DLK1^{high}$ cells and $EpCAM^-DLK1^{low}$ cells in E11.5 liver*

FCM showed that E11.5 liver cells contained at least three populations (Fig. 5A). Because the expression level of DLK1 in $EpCAM^+$ cells is higher than $EpCAM^-$ cells, E11.5 liver could be divided into $EpCAM^+DLK1^{high}$, $EpCAM^-DLK1^{low}$ and $EpCAM^-DLK1^-$ cells. To further examine the feature of

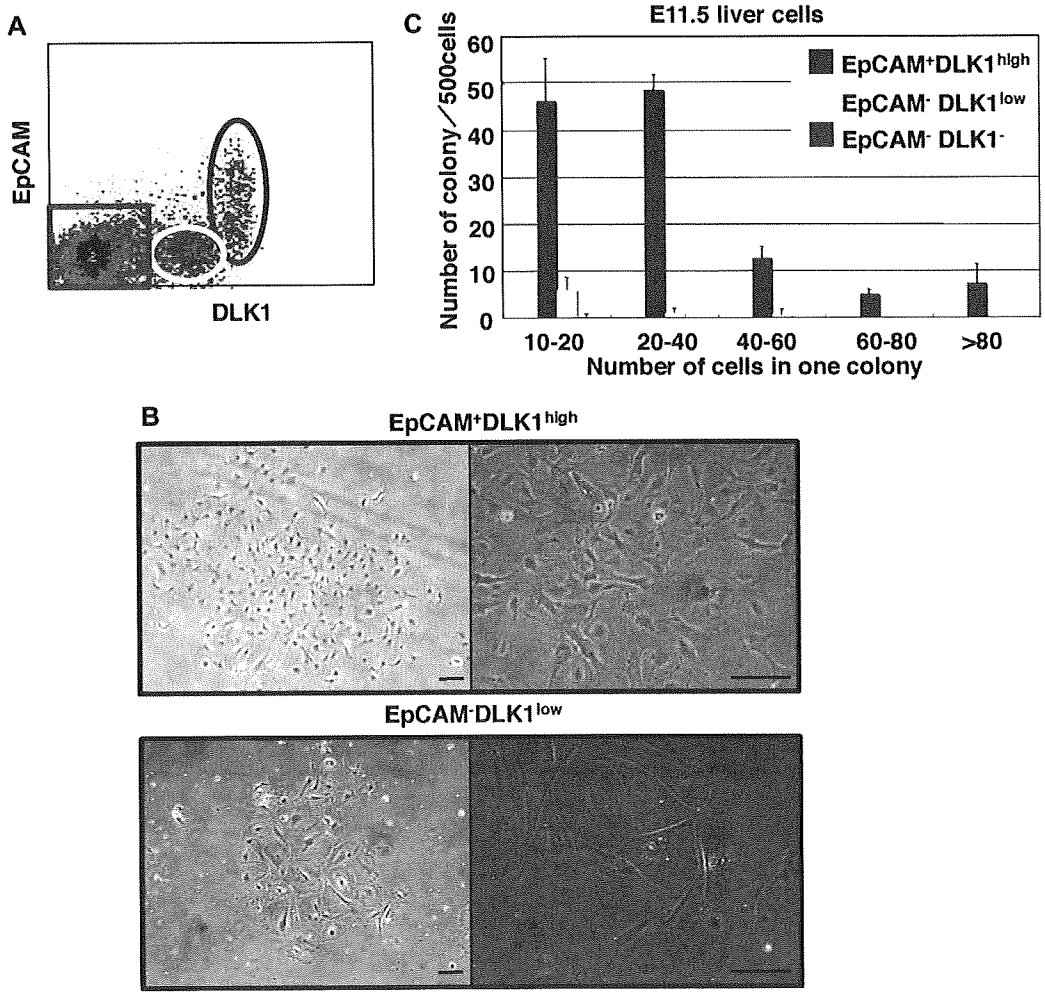

Fig. 5 – Characterization of $EpCAM^+$ and $EpCAM^-$ cells in E11.5. (A) FCM of E11.5 liver cells with anti-DLK1 and anti-EpCAM Abs. (B) Representative morphology of colonies derived from $EpCAM^+DLK1^{high}$ cells (upper panels) and $EpCAM^-DLK1^{low}$ cells (lower panel). Scale bars: 100 μm (C) Colony-forming potential of each cell population isolated from E11.5 liver. $EpCAM^+DLK1^{high}$, $EpCAM^-DLK1^{low}$ and $EpCAM^-DLK1^-$ cells were isolated from E11.5 liver by FACSVantage and each 500 cells were cultured to evaluate colony formation. $EpCAM^+DLK1^{high}$ cells predominantly formed many and large colonies.

hepatoblasts among these cells, we performed in vitro colony formation assays. After 6 days of culture, the number and size of colonies were examined. Approximately 25% of EpCAM$^+$DLK1^{high} cells formed a colony, whereas EpCAM$^-$DLK1^{low} cells formed a small number of colonies and no colony was formed from EpCAM$^-$DLK1$^-$cells (Fig. 5B and C). Moreover, the size of colonies from EpCAM$^+$DLK1^{high} cells was much larger than those from EpCAM$^-$DLK1^{low} cells (Fig. 5C). These results indicated that the expression of EpCAM subdivides DLK1$^+$ cells in E11.5 liver and that it is an excellent marker for early hepatoblasts.

2.5. *Colony formation capacity of EpCAM$^+$DLK1$^+$ cells and EpCAM$^-$DLK1$^+$ cells in E14.5 liver*

It seemed that E14.5 DLK1^{high} hepatoblasts are derived from E11.5 EpCAM$^+$DLK1^{high} cells (Fig. 4). To address this possibility, we performed FCM of E11.5 and E13.5 liver cells with another 40-1 Ab, which binds to unidentified cell-surface protein expressed on hepatoblasts, but not to DLK1 (data not shown). As shown in Fig. 6A, both E11.5 DLK1^{high} cells and E14.5 DLK1^{high} cells maintained high expression levels of the 40-1 antigen, strongly suggesting that the majority of

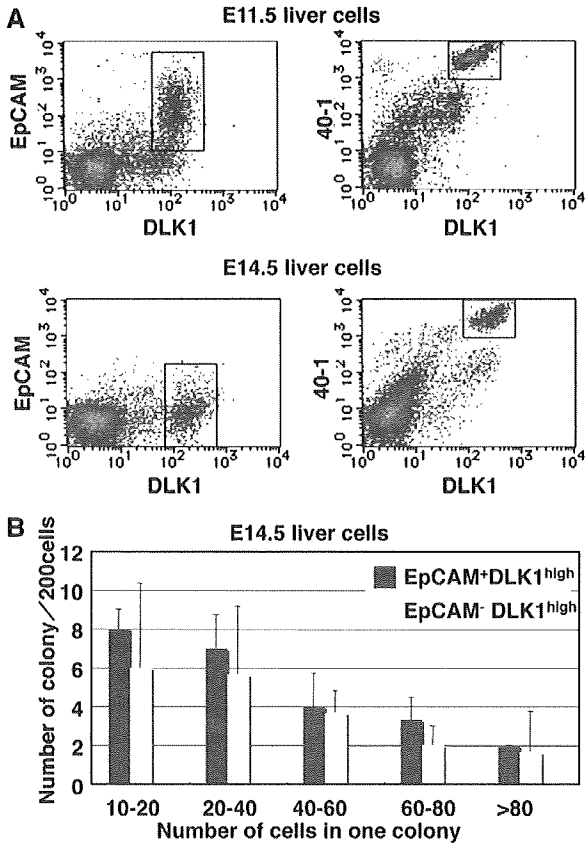

Fig. 6 – Characterization of EpCAM$^{low/+}$DLK1$^+$ cells and EpCAM$^{low/-}$DLK1$^+$ cells isolated from E14.5 liver. (A) FCM of E11.5 and E14.5 liver cells with anti-DLK1, anti-EpCAM and 40-1 antibody. (B) Two hundred cells of either EpCAM$^{low/+}$DLK1$^+$ cells or EpCAM$^{low/-}$DLK1$^+$ cell were cultured to evaluate colony formation. Both types of cells similarly generated many and large colonies.

EpCAM$^+$DLK1^{high} hepatoblasts are losing EpCAM expression to become EpCAM$^-$DLK1^{high} after E12.5.

While highly proliferative hepatoblasts in E11.5 liver were EpCAM$^+$DLK1^{high} cells, there were some E14.5 DLK1^{high} cells with EpCAM at a low expression level (Fig. 4). To compare colony-forming activity between EpCAM$^{low/+}$DLK1^{high} cells and EpCAM$^{low/-}$DLK1^{high} cells in E14.5 liver, we sorted each fraction and performed colony formation assay. Both cell populations showed similar colony-forming activity, including large colonies (Fig. 6B). In addition, the colony-forming capacities of both E11.5 EpCAM$^+$DLK1^{high} and E14.5 EpCAM$^{low/-}$DLK1^{high} cells were comparable. These results supported the possibility that E11.5 EpCAM$^+$DLK1^{high} cells gradually lost EpCAM expression to become EpCAM$^-$DLK1^{high} cells, while further investigation such as genetic lineage tracing will be required for definitive proof. Importantly, DLK1^{high} cells in E14.5 liver include hepatoblasts with high proliferation potential irrespective of EpCAM expression. Thus, EpCAM is the earliest hepatoblast marker but not necessarily a specific marker for hepatoblasts at a later gestational stage in the mouse.

2.6. *Characterization of EpCAM$^+$DLK1^{high} cells and EpCAM$^-$DLK1^{low} cells in E11.5 liver*

We showed that there are at least three major populations, i.e., EpCAM$^+$DLK1^{high}, EpCAM$^-$DLK1^{low} and EpCAM$^-$DLK1$^-$ cells, in E11.5 liver, which displayed quite distinct size and morphology of their colonies in in vitro assays (Fig. 5). To further characterize these three populations, we sorted each cell fraction and compared their gene expression profiles by RT-PCR (Fig. 7A). EpCAM$^+$DLK1^{high} cells expressed various genes that are mainly expressed in hepatoblasts or immature hepatocytes, i.e., albumin, alpha-fetoprotein (AFP), transthyretin (TTR), HNF4α, and c-Met, whereas their expression was weak or hardly detected in EpCAM$^-$DLK1^{low} cells. By contrast, CK19, was highly expressed in EpCAM$^-$DLK1^{low} cells, but was very low in EpCAM$^+$DLK1^{high} cells. EpCAM$^-$DLK1$^-$ cells did not express CK19. Because mouse and rat hepatoblasts do not express CK19, which is a marker for chlolangiocytic differentiation (Shiojiri et al., 1991; Tanimizu et al., 2003), there was a possibility that EpCAM$^+$DLK1^{high} cells contained cells committed to the cholangiocytic lineage. To confirm the results of RT-PCR, we immunostained cytospun cells with anti-albumin and anti-CK19 Abs (Fig. 7B). Consistent with RT-PCR, 86% of EpCAM$^+$DLK1^{high} cells were positive for albumin, whereas 5% of those cells were positive for CK19. On the other hand, 24% and 18% of EpCAM$^-$DLK1^{low} cells were albumin$^+$ and CK19$^+$, respectively. Because intrahepatic bile ducts had not yet been formed at this stage, CK19$^+$ cells could be extrahepatic bile duct cells, gallbladder, or another cell type such as mesothelial cells, which also express CK19. Immunostaining of a sagital section of an E11.5 embryo with anti-CK19 and anti-DLK1 Abs showed that there was an extrahepatic region where DLK1 and CK19 were expressed (Fig. 7C). The CK19$^+$ cells in this region were also stained with *Dolichos biflorus* agglutinin (DBA), which selectively binds to extrahepatic bile ducts (Shiojiri, 1997), indicating that sorted DLK1$^+$ cells included fetal extrahepatic bile duct cells. On the other hand, cells at the mesothelial layer were also positively stained with anti-CK19 (Fig. 7C). These cells were not stained with DBA,

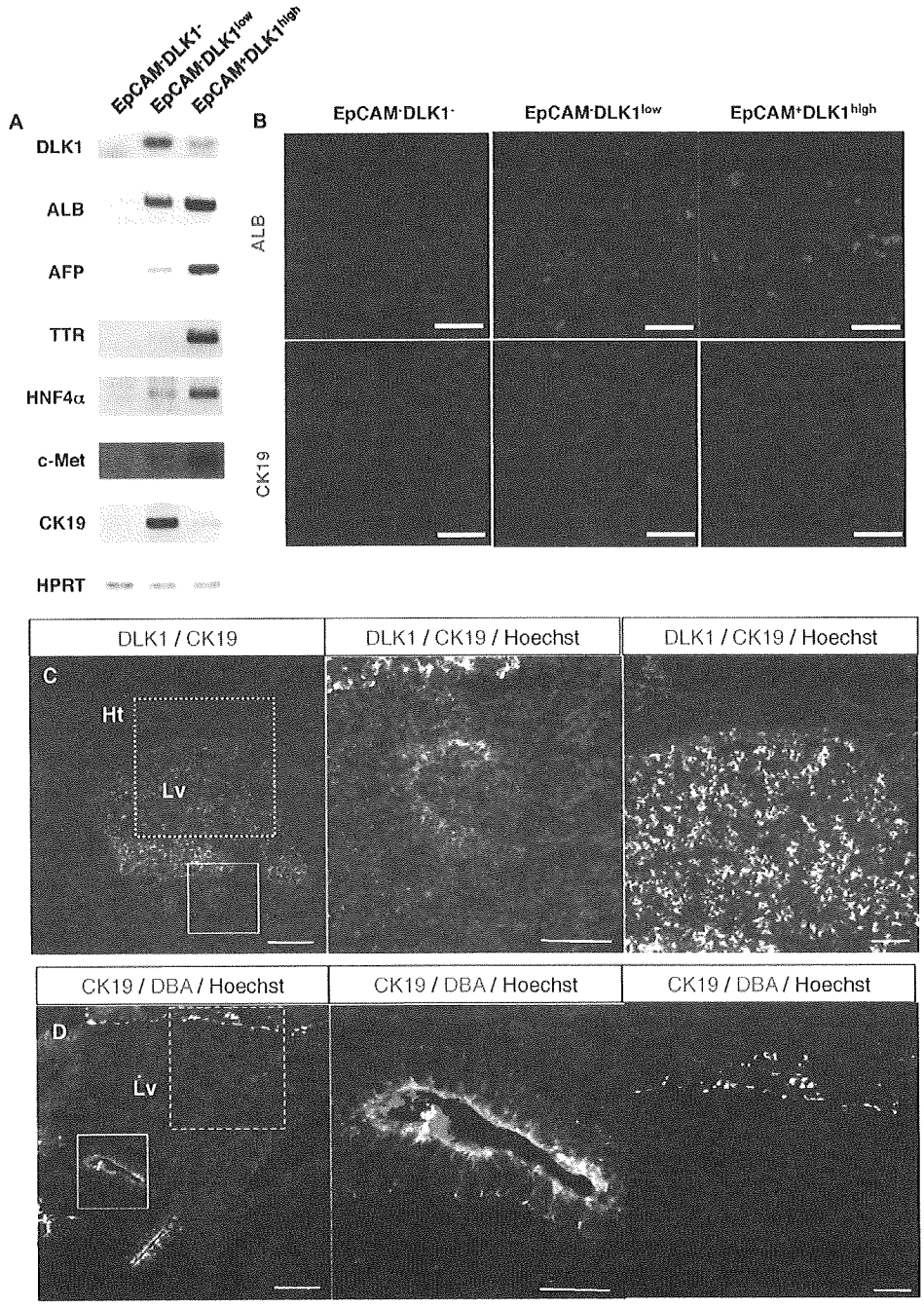

Fig. 7 – Characterization of each population isolated from E11.5 liver by a combination of anti-EpCAM and anti-DLK1 Abs. (A) Gene expression profiles of E11.5 EpCAM^{+}DLK1^{high}, EpCAM^{-}DLK1^{low} and EpCAM^{-}DLK1^{-} cells by RT-PCR. (B) Immunostaining of EpCAM^{+}DLK1^{high}, EpCAM^{-}DLK1^{low} and EpCAM^{-}DLK1^{-} cells with anti-albumin and anti-CK19 Abs by cytospin. (C and D) Immunostaining of a sagital section of an E11.5 embryo with anti-DLK1 and anti-CK19 Ab or DBA. (C, left) The region of the liver primordium is strongly stained with anti-DLK1 Ab. Scale bars: 100 μm. (C, middle) Magnification of the enclosed area by a solid square in the left panel shows that the gallbladder is stained with anti-DLK1 and anti-CK19 Abs. Scale bars: 40 μm. (C, right) Magnification of the enclosed area by a dashed line in the left panel shows that the mesothelium is stained with anti-CK19 Ab. Scale bars: 40 μm. (D, left) The region close to the liver primordium binds DBA. Scale bars: 100 μm. (D, middle) Magnification of the enclosed by a solid square area in the left panel shows that the gallbladder is stained with anti-CK19 Ab and DBA. Scale bars: 40 μm. (D, right) Magnification of the enclosed area by a dotted square area in the left panel shows that the mesothelium is stained with anti-CK19 Ab, but not DBA. Scale bars: 40 μm. (E and F) Staining of E11.5 liver cells with anti-DLK1 and anti-CK19 Abs (E) or DBA-binding by cytospin (F). (G) Staining of E11.5 liver cells with DBA and anti-EpCAM Ab by cytospin. Scale bars: 40 μm. Lv, liver; Ht, heart.

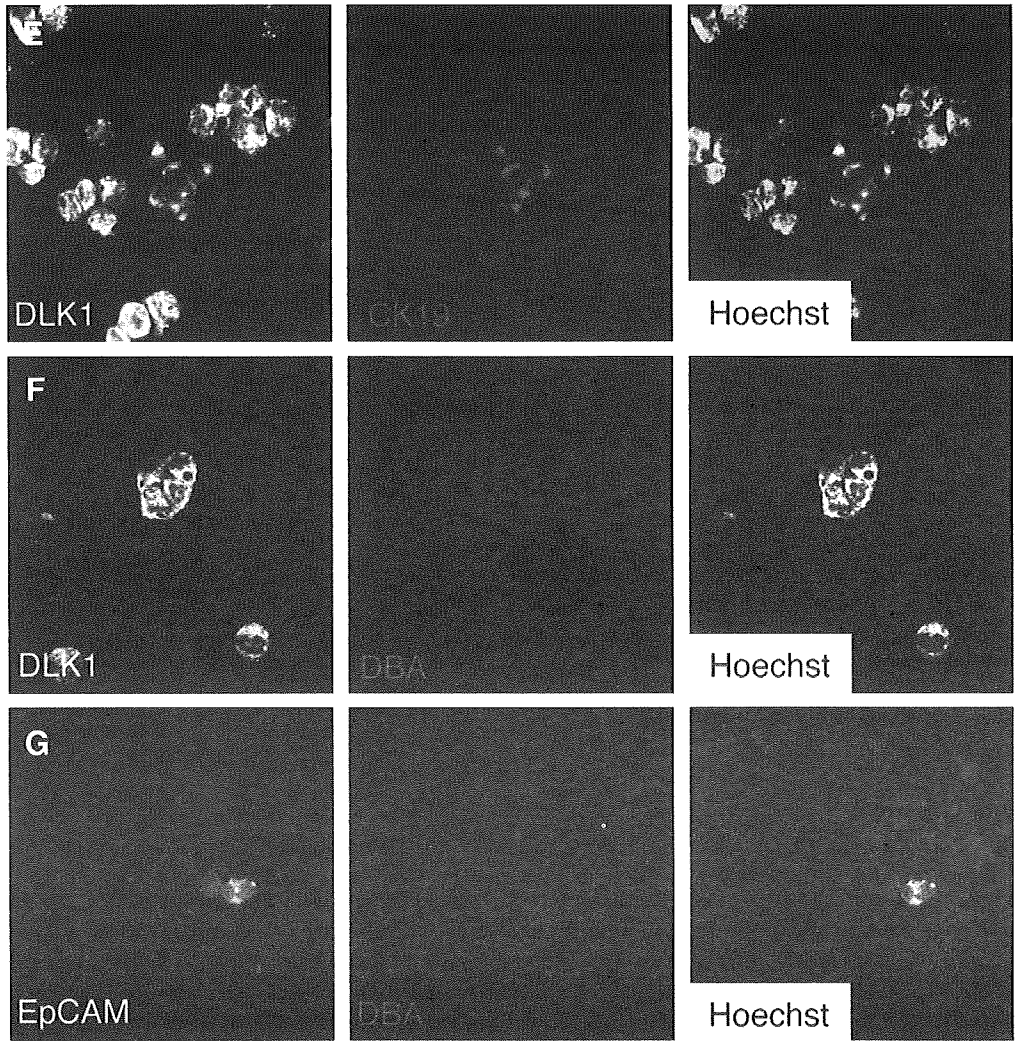

Fig. 7 *(continued)*

indicating that DLK1$^+$ cells also include fetal mesothelial cells (Fig. 7D). The expression of DLK1 in CK19$^+$ cells and DBA$^+$ cells was confirmed by cytospin (Fig. 7E–G). Almost all DBA$^+$ cells were positive for EpCAM, but negative for albumin (data not shown). Therefore, it is likely that low expression of CK19 in EpCAM$^+$DLK1^{high} cells is due to DBA$^+$ extrahepatic bile duct cells. Thus, EpCAM$^-$DLK1^{low} cells in E11.5 liver contain various types of cells, such as low proliferative albumin$^+$ hepatocytes and mesothelial cells. The highly extended morphology of small colonies derived from EpCAM$^-$DLK1^{low} cells is reminiscent of mesothelium (Fig. 5B). In contrast, EpCAM$^+$DLK1^{high} cells contain both highly proliferative hepatoblasts and extrahepatic bile duct cells. Whereas EpCAM$^+$DLK1^{high} hepatoblasts lose the expression of EpCAM along with liver development, extrahepatic bile duct cells will maintain its expression.

Although the liver is a central metabolic organ in adults, it mainly functions as a hematopoietic organ in fetuses. Considering the marked change of liver function from the fetal to adult stage, it is not surprising that the characteristics of hepatoblasts and hepatocytes change during liver development. Whereas E-cadherin and Tim2 are constitutively expressed on the hepatocytic lineage throughout liver development (Nitou et al., 2002; Watanabe et al., 2007), the expression of EpCAM and DLK1 on hepatoblasts is limited at the fetal stage. Therefore, a combination of these markers helps us understand the type of cells and the degree of differentiation. In this report, we show that EpCAM is expressed on hepatoblasts from the onset of liver organogenesis to approximately E14 and also on intrahepatic bile ducts after E16. While DLK1 was previously shown to be expressed on hepatoblasts, our results indicate that DLK1$^+$ cells are further subdivided into EpCAM$^+$ and EpCAM$^-$ cells at an earlier stage. Colony formation assays strongly suggest that EpCAM$^+$DLK1^{high} cells are the earliest and highly proliferative hepatoblasts. Moreover, the expression of EpCAM is markedly downregulated within a short period of time (Fig. 3). Fig. 8 summarizes the expression profiles of marker molecules on hepatic cells during mouse development deduced from these results. Recently, we reported that EpCAM$^+$ cells include potential hepatic stem cells in adult mouse liver (Okabe et al., 2009). It is interesting to know whether EpCAM$^+$ hepatic stem/progenitor cells residing in adult liver are derived from the earliest EpCAM$^+$ hepatoblasts or not. In humans, it has been reported that the multipotent stem/progenitor cells de-

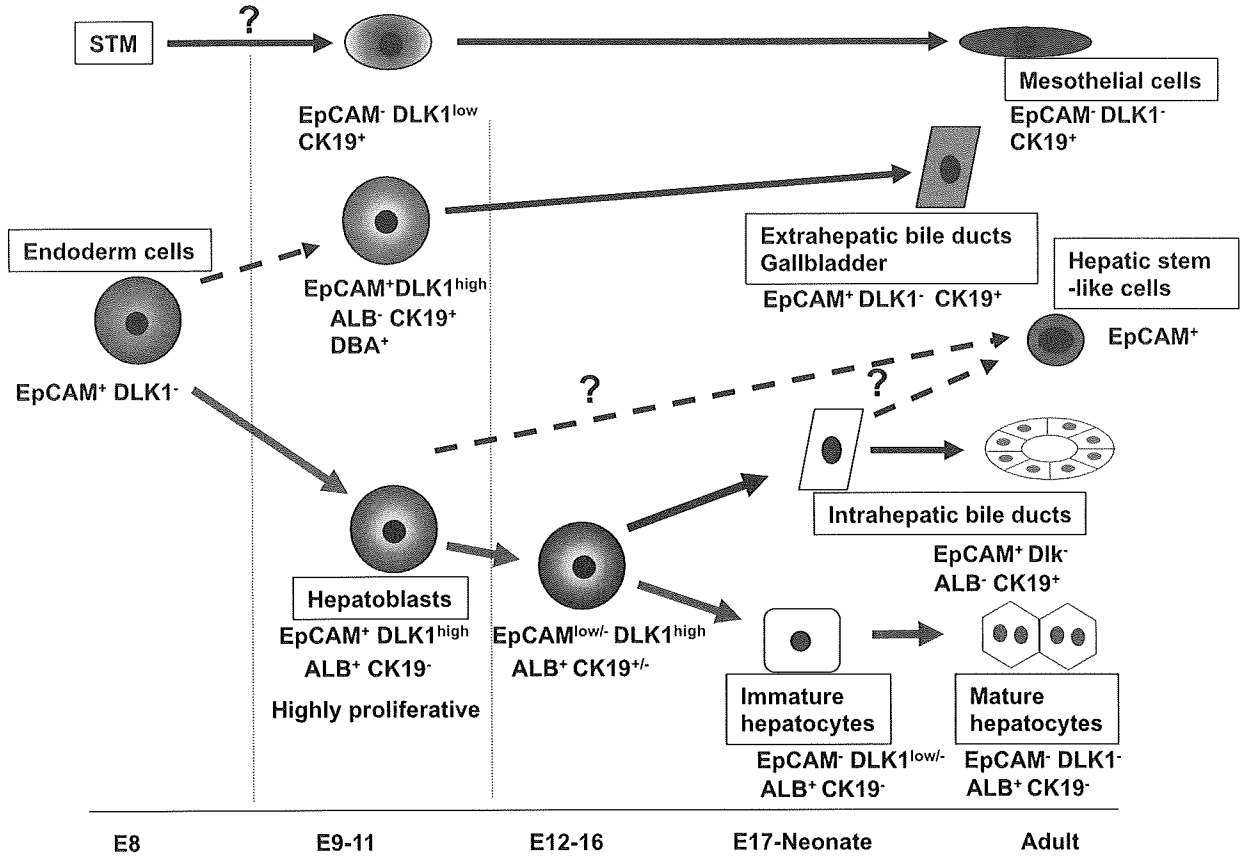

Fig. 8 – Summary of expression profiles of cell-surface markers during mouse liver development. The EpCAM⁺DLK1⁺ hepatoblasts emerged from EpCAM⁺DLK1⁻ foregut endoderm cells form liver bud and migrate into STM at around E9. In E11.5 liver, EpCAM⁺DLK1^{high} cells include highly proliferative hepatoblasts and DBA⁺ extrahepatic bile duct cells. By contrast, EpCAM⁻DLK1^{low} cells include mesothelial precursor cells and immature hepatocytes with low proliferative potential. Thereafter, EpCAM⁺DLK1^{high} hepatoblasts dramatically reduce the expression of EpCAM. At around E16.5, EpCAM is upregulated in ductal plates around a portal vein, while it is absent in hepatoblasts. The origin of EpCAM⁺ adult hepatic stem-like cells is not known at present.

rived from fetal liver express EpCAM (Dan et al., 2006; Schmelzer et al., 2006, 2007). Additionally, it is also reported that approximately 95% and 50% of EpCAM⁺ cells are hepatoblasts in human fetus and neonate, respectively. Because most of mouse hepatoblasts do not express EpCAM at a later gestational stage as described above, it is likely that the characteristics of hepatoblasts in human are somewhat different from those in mouse. In fact, mouse hepatoblasts do not express CK19, whereas human hepatoblasts are known to express CK19 (Stosiek et al., 1990).

In conclusion, we showed that mouse hepatoblasts exhibit a transient expression of EpCAM during liver development and that the combination of DLK1 and EpCAM expression provided evidence for the developmental pathways of mouse liver precursor cells. Defining cell lineages and differentiation stages is a critical step to understand the mechanism of organogenesis. We showed that the earliest mouse hepatoblasts could be identified and isolated prospectively by the expression of EpCAM as early as E11.5. Further investigation on the profile of cell-surface markers will help us to isolate a specific type of precursor cells and to understand mechanisms of each cell differentiation.

3. Materials and methods

3.1. Mice

C57BL/6 mice (Nihon SLC, Hamamatsu, Japan) were used for all experiments. All experiments with animals were performed according to institutional guidelines.

3.2. Antibodies

Anti-DLK1 (24-11) monoclonal antibody (mAb) and 40-1 mAb recognizing hepatoblasts were generated by immunization of a rat with E14.5 mouse fetal liver cells deprived of hematopoietic cells, and screened as previously reported (Suzuki et al., 2008). The anti-DLK1 mAb is commercially available from MBL International (Woburn, MA). The anti-EpCAM mAbs were generated by immunization of a rat with Ba/F3 transfectants expressing mouse EpCAM cDNA (Okabe et al., 2009). Hybridomas expressing mAb were established by fusion of lymphocytes and P3X myeloma cells with polyethyleneglycol as described previously (Hara et al., 1999). Specificity of mAb was confirmed by FCM using Ba/F3 trans-

fectants constitutively expressing mouse EpCAM. Each mAb against DLK1, EpCAM and 40-1 was FITC-labeled or biotinylated and used for FCM. The rabbit anti-mouse CK19 polyclonal Ab was raised against the C-terminal peptide, HYNNLPTPKAI, and the serum was used for immunostaining, as previously described (Tanimizu et al., 2003). Rhodamine *Dolichos biflorus* agglutinin was purchased from Vector Labolatories (Burlingame, CA). Anti-HNF4α Ab (H-171) (Santa Cruz Biotechnology) and anti-mouse CD326 (EpCAM) (G8.8) (BD Pharmingen) were used for IHC.

3.3. *Immunohistochemistry*

Whole embryos or fetal liver were fixed by incubation in a 4% paraformaldehyde solution at 4 °C overnight, followed by dehydration sequentially in 15% sucrose and 30% sucrose solution overnight, and then embedded in OCT. Cryostat sections (7 μm) were incubated with each Ab, followed by a biotin- or fluorescein-conjugated secondary Ab. The signals were visualized using the Vectastain ABC Elite kit (Vector Laboratories, Burlingame, CA) or fluorescence microscopy. Primary Abs used were: anti-EpCAM 1:200 (BD Pharmingen, San Diego, CA); anti-DLK1 1:200 (MBL); anti-CK19 1:1000. Secondary Abs used were conjugated to FITC or PE (BD Pharmingen).

3.4. *Preparation and isolation of liver cells*

Fetal liver cells were prepared according to the method of Kamiya et al. (1999) These cells were used for FCM analysis and isolation of $EpCAM^+$ cells. $EpCAM^+$ cells were isolated using AutoMACS according to the manufacturer's instructions (Miltenyi Biotec, Bergisch Gladbach, Germany). Briefly, E11.5 liver cells were incubated with anti-FcR Ab for the block of FcR, and then incubated with FITC-conjugated anti-EpCAM mAb. After washing with phosphate-buffered saline (PBS), cells were resuspended in AutoMACS running buffer, and 100 μl/ml of anti-FITC-labeled microbeads (Miltenyi Biotec) were added. After washing with the running buffer, the cells were loaded onto a magnetic column and $EpCAM^+$ cells were eluted from the column after the depletion of $EpCAM^-$ cells. Positive and negative selections were performed twice to prepare $EpCAM^+$ cells and $EpCAM^-$ cells. The purity of each population was over 90%. $EpCAM^+DLK1^+$, $EpCAM^-DLK1^+$ and $EpCAM^-DLK1^-$ cells from E11.5 liver were isolated by FACSVantage using FITC-conjugated anti-DLK1 mAb, biotinylated anti-EpCAM mAb and streptavidin-APC. Dead cells were excluded by propidium iodide (1 μg/mL) staining and FL-3 gating.

3.5. *Colony formation assay*

Fetal liver cells were cultured as previously described (Tanimizu et al., 2003). Briefly, cells were plated at 50 cells/cm^2 in DMEM/F12 medium supplemented with10% FBS, 1× ITS, 10 mM nicotineamide (Wako, Tokyo, Japan), 0.1 mM dexamethasone, 5 mM L-glutamine, 20 ng/ml EGF (PeproTech, London, UK), and 20 ng/ml HGF (R&D, Minneapolis, MN) on a type I collagen-coated dish. After 6 days of culture, the number of colonies was determined.

3.6. *RNA extraction and reverse transcriptase polymerase chain reaction (RT-PCR)*

Total RNA was extracted from each cell preparation with Trizol reagent (Invitrogen, Carlsbad, CA). Total RNA and random hexamer primers were used to synthesize cDNA using the First-strand cDNA synthesis kit (Amersham Pharmacia Biotech, Piscataway, NJ). The PCR primers and conditions are described below: the samples were denatured at 95 °C for 20 s, followed by 30–40 thermal cycles; denaturation at 95 °C for 10 s, annealing at 56 °C for 20 s, and extension at 72 °C for 90 s, with a final extension at 72 °C for 5 min. PCR primers of albumin, AFP, HNF4α, CK19 were described previously (Tanimizu et al., 2003). The other primers used are: TTR (5′-atccacaagctcctgacag-3′ and 5′-actgctttggcaagatcctgg-3′), c-Met (5′-ggaagagggcattttggctg-3′ and 5′-agcacaccgaaggaccacac-3′), HPRT (5′-gactgaaagacttgctcgag-3′ and 5′-ccagcaagcttgcaaccttaacaa-3′). The real-time PCR for EpCAM was performed using LightCycler (Roche) according to manufacturer's protocol. The used primers of EpCAM were 5′-aggggcgatccagaacaacg-3′ and 5′-atggtcgtaggggctttctc-3′.

Acknowledgements

This work was supported in part by a grant for Promotion of Independence for Young Investigators of Japan Science and Technology Agency (JST), and a Grant-in-Aid for Scientific Research and Global COE Program from the Ministry of Education, Sports, Science and Technology, Japan.

REFERENCES

Armstrong, A., Eck, S.L., 2003. EpCAM: a new therapeutic target for an old cancer antigen. Cancer Biol. Ther. 2, 320–326.

Dabeva, M.D., Shafritz, D.A., 1993. Activation, proliferation, and differentiation of progenitor cells into hepatocytes in the D-galactosamine model of liver regeneration. Am. J. Pathol. 143, 1606–1620.

Dan, Y.Y., Riehle, K.J., Lazaro, C., Teoh, N., Haque, J., Campbell, J.S., Fausto, N., 2006. Isolation of multipotent progenitor cells from human fetal liver capable of differentiating into liver and mesenchymal lineages. Proc. Natl. Acad. Sci. USA 103, 9912–9917.

de Boer, C.J., van Krieken, J.H., Janssen-van Rhijn, C.M., Litvinov, S.V., 1999. Expression of Ep-CAM in normal, regenerating, metaplastic, and neoplastic liver. J. Pathol. 188, 201–206.

Douarin, N.M., 1975. An experimental analysis of liver development. Med. Biol. 53, 427–455.

Evarts, R.P., Nakatsukasa, H., Marsden, E.R., Hsia, C.C., Dunsford, H.A., Thorgeirsson, S.S., 1990. Cellular and molecular changes in the early stages of chemical hepatocarcinogenesis in the rat. Cancer Res. 50, 3439–3444.

Fausto, N., Lemire, J.M., Shiojiri, N., 1993. Cell lineages in hepatic development and the identification of progenitor cells in normal and injured liver. Proc. Soc. Exp. Biol. Med. 204, 237–241.

Germain, L., Blouin, M.J., Marceau, N., 1988. Biliary epithelial and hepatocytic cell lineage relationships in embryonic rat liver as determined by the differential expression of cytokeratins, alpha-fetoprotein, albumin, and cell surface-exposed components. Cancer Res. 48, 4909–4918.

Gualdi, R., Bossard, P., Zheng, M., Hamada, Y., Coleman, J.R., Zaret, K.S., 1996. Hepatic specification of the gut endoderm in vitro: cell signaling and transcriptional control. Genes Dev. 10, 1670–1682.

Hara, T., Nakano, Y., Tanaka, M., Tamura, K., Sekiguchi, T., Minehata, K., Copeland, N.G., Jenkins, N.A., Okabe, M., Kogo, H., Mukouyama, Y., Miyajima, A., 1999. Identification of podocalyxin-like protein 1 as a novel cell surface marker for hemangioblasts in the murine aorta-gonad-mesonephros region. Immunity 11, 567–578.

Hreha, G., Jefferson, D.M., Yu, C.H., Grubman, S.A., Alsabeh, R., Geller, S.A., Vierling, J.M., 1999. Immortalized intrahepatic mouse biliary epithelial cells: immunologic characterization and immunogenicity. Hepatology 30, 358–371.

Jensen, C.H., Jauho, E.I., Santoni-Rugiu, E., Holmskov, U., Teisner, B., Tygstrup, N., Bisgaard, H.C., 2004. Transit-amplifying ductular (oval) cells and their hepatocytic progeny are characterized by a novel and distinctive expression of delta-like protein/preadipocyte factor 1/fetal antigen 1. Am. J. Pathol. 164, 1347–1359.

Jung, J., Zheng, M., Goldfarb, M., Zaret, K.S., 1999. Initiation of mammalian liver development from endoderm by fibroblast growth factors. Science 284, 1998–2003.

Kamiya, A., Kinoshita, T., Ito, Y., Matsui, T., Morikawa, Y., Senba, E., Nakashima, K., Taga, T., Yoshida, K., Kishimoto, T., Miyajima, A., 1999. Fetal liver development requires a paracrine action of oncostatin M through the gp130 signal transducer. EMBO J. 18, 2127–2136.

Kubota, H., Reid, L.M., 2000. Clonogenic hepatoblasts, common precursors for hepatocytic and biliary lineages, are lacking classical major histocompatibility complex class I antigen. Proc. Natl. Acad. Sci. USA 97, 12132–12137.

Lemaigre, F.P., 2003. Development of the biliary tract. Mech. Dev. 120, 81–87.

Matsumoto, K., Yoshitomi, H., Rossant, J., Zaret, K.S., 2001. Liver organogenesis promoted by endothelial cells prior to vascular function. Science 294, 559–563.

Minguet, S., Cortegano, I., Gonzalo, P., Martinez-Marin, J.A., de Andres, B., Salas, C., Melero, D., Gaspar, M.L., Marcos, M.A., 2003. A population of c-Kit(low)(CD45/TER119)- hepatic cell progenitors of 11-day postcoitus mouse embryo liver reconstitutes cell-depleted liver organoids. J. Clin. Invest. 112, 1152–1163.

Momburg, F., Moldenhauer, G., Hammerling, G.J., Moller, P., 1987. Immunohistochemical study of the expression of a Mr 34, 000 human epithelium-specific surface glycoprotein in normal and malignant tissues. Cancer Res. 47, 2883–2891.

Nitou, M., Sugiyama, Y., Ishikawa, K., Shiojiri, N., 2002. Purification of fetal mouse hepatoblasts by magnetic beads coated with monoclonal anti-e-cadherin antibodies and their in vitro culture. Exp. Cell Res. 279, 330–343.

Okabe, M., Tsukahara, Y., Tanaka, M., Suzuki, K., Saito, S., Kamiya, Y., Tsujimura, T., Nakamura, K., Miyajima, A., 2009. Potential hepatic stem cells reside in EpCAM+ cells of normal and injured mouse liver. Development 136, 1951–1960.

Rogler, L.E., 1997. Selective bipotential differentiation of mouse embryonic hepatoblasts in vitro. Am. J. Pathol. 150, 591–602.

Rossi, J.M., Dunn, N.R., Hogan, B.L., Zaret, K.S., 2001. Distinct mesodermal signals, including BMPs from the septum transversum mesenchyme, are required in combination for hepatogenesis from the endoderm. Genes Dev. 15, 1998–2009.

Schmelzer, E., Wauthier, E., Reid, L.M., 2006. The phenotypes of pluripotent human hepatic progenitors. Stem Cells 24, 1852–1858.

Schmelzer, E., Zhang, L., Bruce, A., Wauthier, E., Ludlow, J., Yao, H.L., Moss, N., Melhem, A., McClelland, R., Turner, W., Kulik, M., Sherwood, S., Tallheden, T., Cheng, N., Furth, M.E., Reid, L.M., 2007. Human hepatic stem cells from fetal and postnatal donors. J. Exp. Med. 204, 1973–1987.

Sell, S., 1990. Is there a liver stem cell? Cancer Res. 50, 3811–3815.

Shiojiri, N., 1994. Transient expression of bile-duct-specific cytokeratin in fetal mouse hepatocytes. Cell Tissue Res. 278, 117–123.

Shiojiri, N., 1997. Development and differentiation of bile ducts in the mammalian liver. Microsc. Res. Tech. 39, 328–335.

Shiojiri, N., Lemire, J.M., Fausto, N., 1991. Cell lineages and oval cell progenitors in rat liver development. Cancer Res. 51, 2611–2620.

Sosa-Pineda, B., Wigle, J.T., Oliver, G., 2000. Hepatocyte migration during liver development requires Prox1. Nat. Genet. 25, 254–255.

Spagnoli, F.M., Amicone, L., Tripodi, M., Weiss, M.C., 1998. Identification of a bipotential precursor cell in hepatic cell lines derived from transgenic mice expressing cyto-Met in the liver. J. Cell Biol. 143, 1101–1112.

Stosiek, P., Kasper, M., Karsten, U., 1990. Expression of cytokeratin 19 during human liver organogenesis. Liver 10, 59–63.

Suzuki, A., Zheng, Y., Kondo, R., Kusakabe, M., Takada, Y., Fukao, K., Nakauchi, H., Taniguchi, H., 2000. Flow-cytometric separation and enrichment of hepatic progenitor cells in the developing mouse liver. Hepatology 32, 1230–1239.

Suzuki, K., Tanaka, M., Watanabe, N., Saito, S., Nonaka, H., Miyajima, A., 2008. p75 Neurotrophin receptor is a marker for precursors of stellate cells and portal fibroblasts in mouse fetal liver. Gastroenterology 135, 270–281. e3.

Tanimizu, N., Nishikawa, M., Saito, H., Tsujimura, T., Miyajima, A., 2003. Isolation of hepatoblasts based on the expression of Dlk/Pref-1. J. Cell Sci. 116, 1775–1786.

Tanimizu, N., Tsujimura, T., Takahide, K., Kodama, T., Nakamura, K., Miyajima, A., 2004. Expression of Dlk/Pref-1 defines a subpopulation in the oval cell compartment of rat liver. Gene Expr. Patterns 5, 209–218.

Thorgeirsson, S.S., Evarts, R.P., Bisgaard, H.C., Fujio, K., Hu, Z., 1993. Hepatic stem cell compartment: activation and lineage commitment. Proc. Soc. Exp. Biol. Med. 204, 253–260.

Tian, Y.W., Smith, P.G., Yeoh, G.C., 1997. The oval-shaped cell as a candidate for a liver stem cell in embryonic, neonatal and precancerous liver: identification based on morphology and immunohistochemical staining for albumin and pyruvate kinase isoenzyme expression. Histochem. Cell Biol. 107, 243–250.

Watanabe, N., Tanaka, M., Suzuki, K., Kumanogoh, A., Kikutani, H., Miyajima, A., 2007. Tim2 is expressed in mouse fetal hepatocytes and regulates their differentiation. Hepatology 45, 1240–1249.

Yovchev, M.I., Grozdanov, P.N., Zhou, H., Racherla, H., Guha, C., Dabeva, M.D., 2008. Identification of adult hepatic progenitor cells capable of repopulating injured rat liver. Hepatology 47, 636–647.

Zaret, K., 1998. Early liver differentiation: genetic potentiation and multilevel growth control. Curr. Opin. Genet. Dev. 8, 526–531.

EXPERIMENTAL CELL RESEARCH 315 (2009) 2648–2657

available at www.sciencedirect.com

ScienceDirect

www.elsevier.com/locate/yexcr

Research Article

Hedgehog signal activation coordinates proliferation and differentiation of fetal liver progenitor cells☆

Yoshikazu Hirose, Tohru Itoh, Atsushi Miyajima*

Laboratory of Cell Growth and Differentiation, Institute of Molecular and Cellular Biosciences, The University of Tokyo, 1-1-1 Yayoi, Bunkyo-ku, Tokyo 113-0032, Japan

ARTICLE INFORMATION

Article Chronology:
Received 25 February 2009
Revised version received 11 May 2009
Accepted 16 June 2009
Available online 24 June 2009

Keywords:
Hedgehog signaling
Fetal liver
Hepatoblast

ABSTRACT

Hedgehog (Hh) signaling plays crucial roles in development and homeostasis of various organs. In the adult liver, it regulates proliferation and/or viability of several types of cells, particularly under injured conditions, and is also implicated in stem/progenitor cell maintenance. However, the role of this signaling pathway during the normal developmental process of the liver remains elusive. Although *Sonic hedgehog* (*Shh*) is expressed in the ventral foregut endoderm from which the liver derives, the expression disappears at the onset of the liver bud formation, and its possible recurrence at the later stages has not been investigated. Here we analyzed the activation and functional relevance of Hh signaling during the mouse fetal liver development. At E11.5, *Shh* and an activation marker gene for Hh signaling, *Gli1*, were expressed in Dlk^+ hepatoblasts, the fetal liver progenitor cells, and the expression was rapidly decreased thereafter as the development proceeded. In the culture of Dlk^+ hepatoblasts isolated from the E11.5 liver, activation of Hh signaling stimulated their proliferation and this effect was cancelled by a chemical Hh signaling inhibitor, cyclopamine. In contrast, hepatocyte differentiation of Dlk^+ hepatoblasts *in vitro* as manifested by the marker gene expression and acquisition of ammonia clearance activity was significantly inhibited by forced activation of Hh signaling. Taken together, these results demonstrate the temporally restricted manner of Hh signal activation and its role in promoting the hepatoblast proliferation, and further suggest that the pathway needs to be shut off for the subsequent hepatic differentiation of hepatoblasts to proceed normally.

Introduction

The liver is the largest organ in the adult human body and plays a central role in metabolism, serum protein synthesis, detoxification and the maintenance of systemic homeostasis. It is composed of many types of cells including hepatocytes, the parenchymal component executing the majority of the organ's functions, and other non-parenchymal cells such as cholangiocytes, Kupffer cells, hepatic stellate cells (HSCs), and endothelial cells. Among those cell types, hepatocytes and cholangiocytes, the two epithelial lineages in the organ, derive from a common precursor cell population in the developing liver [1]. Elucidating the nature and the regulatory mechanisms of these hepatic progenitor cells, so-called hepatoblasts, is a fundamental issue to understand how liver architecture and function are properly manufactured.

Liver organogenesis starts at embryonic day (E) 8.5 in the mouse, when liver diverticulum is formed from the ventral foregut endoderm in response to fibroblast growth factor (FGF), secreted

☆ This work was supported in part by Grants-in-Aid for Scientific Research from the Ministry of Education, Culture, Sports, Science and Technology of Japan (17014016) and from the CREST program of Japan Science and Technology Agency.

* *Corresponding author.* Fax: +81 3 5841 8475.
E-mail address: itohru@iam.u-tokyo.ac.jp (T. Itoh).

0014-4827/$ – see front matter © 2009 Elsevier Inc. All rights reserved.
doi:10.1016/j.yexcr.2009.06.018

from the cardiac mesoderm, and bone morphogenetic protein (BMP), secreted from the septum transversum mesenchyme (STM) [1–4]. Hepatoblasts emerging from the ventral endodermal epithelium proliferate by the help of endothelial cells and form the liver bud [5]. Proliferation of hepatoblasts is known to be regulated by various extracellular signals, such as hepatocyte growth factor (HGF) [6], transforming growth factor β (TGFβ) [7] and Wnt [8]. Around E10, hematopoietic cells immigrate into the fetal liver from the aorta–gonad–mesonephros region and the placenta, and expand their population tremendously in the microenvironment provided by the fetal liver till birth. During this period of time, hematopoietic cells enhance differentiation of hepatoblasts into hepatocytes by producing cytokines [9]. As hematopoiesis switches from the fetal liver to the bone marrow, liver organogenesis progresses to become a center for metabolism. In this process, hepatocyte differentiation is enhanced by oncostatin M (OSM) [10], HGF [11] and extracellular matrices (ECMs) [12].

The *Hedgehog* (*Hh*) gene, initially identified from a genetic screen in *Drosophila melanogaster*, encodes a secreted factor with multiple biological activities, ranging from regulation of cell proliferation and differentiation to pattern formation as a morphogen [13,14]. In mammals there are three Hh orthologs, namely Sonic hedgehog (Shh), Indian hedgehog (Ihh) and Desert hedgehog (Dhh). Hh is synthesized as a ~45 kDa precursor protein and cleaved to generate the biologically active amino-terminal Hh signaling domain (HhN). In the absence of Hh ligands, the Hh receptor Patched (Ptc) inhibits the activity of another membrane-bound protein, Smoothened (Smo) [15,16]. Binding of Hh to Ptc inactivates its inhibitory effect toward Smo, thereby releasing Smo activity to emanate downstream signals. The Glioblastoma (Gli) family of transcription factors constitutes the key components of the pathway activated by Smo, which then enters the nucleus and stimulates transcription of multiple target genes, including *Gli1* and *Ptc1*, to control multiple cellular functions. Through its range of biological activities, Hh signaling plays crucial roles in development of many fetal tissues and organs, and also in homeostasis of adult tissues by maintaining tissue stem/progenitor cells [17,18]. Notably, aberrant activation of Hh signaling is often associated with formation of multiple types of solid tumors, including hepatocellular carcinoma, cholangiocarcinoma and hepatoblastoma in the liver [19–21].

With regard to the liver, many studies to date have already implicated Hh signaling in adults under several pathological conditions. For instance, HSCs, bile ductular cells and fibroblastic cells express Hh related genes to regulate proliferation and viability of these cells when the liver is damaged [20,22–24]. On the other hand, whether and how the signaling is involved in developmental process of the organ remains little investigated. While *Shh* is initially expressed broadly in the ventral foregut endoderm in mouse embryos around E8.5, its expression becomes lost in the hepatic endoderm at E9.0–9.5, the region which subsequently forms the liver bud [25–28]. Indeed, a study using *Hex* knockout mice has implied that the *Shh* expression needs to be shut off at this stage for the liver bud formation and hepatoblast development to proceed normally [28]. Although expression of Shh as well as other Hh ligands at later stages during liver development has not been directly addressed, it is of interest to note that, in the *Ptc-lacZ* knock-in mice that express lacZ under the control of the Hh-responsive *Ptc* promoter activity, some lacZ signals can be detected in the fetal liver at E11.5 [29], indicating possible activation and functional implication of Hh signaling therein.

In this paper, we address a possible functional involvement of Hh signaling in mouse fetal liver organogenesis. Our results have demonstrated temporally restricted and cell type-specific patterns of ligand expression and pathway activation, and their functional impact on hepatoblast regulation.

Materials and methods

Mice

C57BL/6 mice were purchased from Nihon SLC (Shizuoka, Japan). All procedures were performed according to the guideline set by the institutional animal care and use committee of the University of Tokyo.

Isolation of Dlk$^+$ fetal liver cells by magnetic cell sorter (MACS)

Mouse Dlk$^+$ fetal liver cells were obtained according to the methods by Kamiya et al. [10] and Tanimizu et al. [30]. Briefly, mouse fetal livers were dissociated with liver digestion medium (Gibco) followed by hemolysis with a hypotonic buffer. Dissociated cells were incubated with biotinylated anti-Dlk antibody [31]. After a wash, cells were incubated with streptavidin-labeled microbeads (Miltenyi Biotec) and isolated by an automatic magnetic cell sorter (AutoMACS; Miltenyi Biotec).

Fluorescence-activated cell sorting (FACS)

E11.5 mouse fetal livers were dissociated according to the method described above. Dissociated cells were incubated with antibodies and sorted by the FACS-Vantage system (Becton Dickinson Biosciences). Anti-p75NTR antibody and anti-mouse Dlk antibody were generated by Suzuki et al. [31], and anti-Stab2 antibody by Nonaka et al. [32]. Signals were fluoresced using Alexa Fluor 488-conjugated anti-rat IgG (Invitrogen) and Alexa Fluor 647-conjugated anti-rat IgG (Invitrogen). Phycoerythrin (PE)-conjugated anti-CD45 (553081), fluorescein isothiocyanate (FITC)-conjugated anti-Ter119 (557915) and PE-conjugated anti-Ter119 (553673) were purchased from BD biosciences. Dead cells were stained with propidium iodide (PI).

Real-time RT-PCR

Total RNA samples were isolated with TRIzol reagent (Invitrogen). Reverse transcription to cDNA templates was performed using random primers and Superscript III reverse transcriptase (Invitrogen). Real-time RT-PCR experiments were conducted by use of a LightCycler (Roche Diagnostics) and SYBR Premix Ex Taq (Takara-bio). Primers for *Glyceraldehyde-3-phosphate dehydrogenase* (*Gapdh*) were used as the normalization control. The pairs of primers used were as follows: 5′-TGAACGGGAAGTCACTGG-3′ (*Gapdh* primer, sense), 5′-TCCACCACCCTGTTGCTGTA-3′ (*Gapdh* primer, antisense), 5′-CCAAGCCAACTTTATGTCAGGG-3′ (*Gli1* primer, sense), 5′-AGCCC-GCTTCTTTGTTAATTTGA-3′ (*Gli1* primer, antisense), 5′-CCAATTACA-ACCCCGACATC-3′ (*Shh* primer, sense), 5′-GCATTTAACTTGTCTTTGC-ACCT-3′ (*Shh* primer, antisense), 5′-TGCATTGCTCTGTCAAGTCTG-3′ (*Ihh* primer, sense), 5′-GCTCCCCGTTCTCTAGGC-3′ (*Ihh* primer, antisense), 5′-CATCTGGAGCCATGTACCTT-3′ (*Tat* primer, sense),

5′-TCCAGCATCATCACCTCG-3′ (*Tat* primer, antisense), 5′-GGCTGG-CTACCAAGAGTCTG-3′ (*Cps1* primer, sense), 5′-TGTATCCACTCCAT-AAATTGCAG-3′ (*Cps1* primer, antisense).

Immunocytochemistry

Dlk^+ and Dlk^- fetal liver cells isolated using MACS were mounted on glass slides by cytospinning and fixed using 4% paraformaldehyde (PFA). Cultured Dlk^+ cells were fixed using 4% PFA at day 7. Fixed cells were treated with L.A.B. solution (Polysciences) at room temperature for 10 min for antigen retrieval, and then incubated with anti-Dlk antibody, anti-Gli1 antibody (Chemicon) and anti-Ki67 antibody (BD Pharmigen). Signals were visualized using Alexa Fluor 488-conjugated anti-rat IgG (Invitrogen), Alexa Fluor 555-conjugated anti-rabbit IgG (Invitrogen) and Alexa Fluor 488-conjugated anti-mouse IgG (invitrogen), respectively, and observed under a fluorescence microscope. Nuclei were counterstained with Hoechst33342 (Sigma). In the cultured samples, $Ki67^+$ cells and nuclei were manually counted under a fluorescence microscope in three independent fields.

Culture of Dlk^+ cells

Dlk^+ fetal liver cells were resuspended in Dulbecco's Modified Eagle Medium (DMEM; Gibco) containing 10% fetal bovine serum (FBS; JRH), 2 mM L-glutamine (Gibco), 1× nonessential amino acid solution (Gibco), 1× insulin/transferrin/selenium (ITS; Gibco), 50 μg/ml of gentamicin, 10^{-7} M of dexamethasone (Dex; Sigma), and 10 ng/ml of murine OSM (R&D systems). Cells were plated at 2.1×10^4 cells/cm^2 on gelatin-coated dishes. Recombinant N-terminus of Shh (ShhN; R&D systems), 2 μM purmorphamine (Wako Pure Chemical Industries), 0.1% of ethanol (EtOH) and 5 μM of cyclopamine (Wako Pure Chemical Industries) were added where indicated. ShhN was used at a final concentration of 0.5 μg/ml except for Supplementary Fig. 2. Culture media were replaced every 2 days.

Quantification of cell proliferation

Cell proliferation was quantified by using the cell proliferation reagent WST-1 (Roche Diagnostics) according to the manufacturer's instructions. Dlk^+ cells were cultured in 96-well microplates at the same density as above with 100 μl/well of media. Culture media were replaced every 2 days. After 7 days of culture, 10 μl of WST-1 was added to each well and the cells were further incubated for about 1 h. The optical absorbance of the samples was measured at 450 nm.

Colony formation assay

Dlk^+ cells from E11.5 fetal livers were resuspended in DMEM/F12 (Gibco) containing 10% FBS, 10 mM nicotinamide, 5 mM L-glutamine, 1× ITS, 10 ng/ml of murine epidermal growth factor (Peprotech), 10 ng/ml of human HGF (Peprotech), 50 μg/ml of gentamicin, and 10^{-7} M Dex. Five hundred cells per well were plated on collagen-coated 6-well plates. At day 3, equal amount of fresh media was added. After cultivation for 6 days, cells were fixed with 4% PFA and dried up. Cell numbers and colony sizes were manually counted under microscopic observation.

Measurement of ammonia concentrations

Ammonia concentration was measured as previously described [33]. Briefly, culture media were replaced with fresh media containing 2 mM of NH_4Cl at day 10. Cells were further incubated for 48 h, and the culture media were subjected to analyses at various time points by the modified indophenol method using Ammonia-test Wako (Wako Pure Chemical Industries).

Statistics

Data are presented as the mean plus standard error (SE). Statistical significance was assessed by means of a Student's *T* test. A *P* value less than 0.05 was considered statistically significant.

Results

Hh signaling is transiently activated in E11.5 hepatoblasts

In a previous study using the *Ptc-LacZ* mice, where Hh signal activation can be monitored *in situ* by the LacZ reporter expression, some positive signals were observed in the liver of E11.5 mouse embryos [29], indicating that Hh signaling may be operating in the fetal liver at this stage. However, the nature of the Hh-responsive cell(s) as well as activation of the signaling at other developmental stages is not precisely clarified. Thus, we set out to investigate expression of *Hh* genes during the course of fetal liver development by real-time RT-PCR analyses using whole liver samples. As shown in Fig. 1A, expression of *Shh* was evident at E11.5, and decreased gradually as the development proceeded. Accordingly, *Gli1*, a direct transcriptional target of Hh signaling, showed a similar expression pattern. By contrast, expression of *Ihh* increased toward the birth, and then dramatically decreased thereafter. *Dhh* was not detected in these samples (data not shown), consistent with the notion that it is mainly expressed in the testis and Schwann cells [34,35].

As Hh signaling has been implicated in maintenance of hepatic stem/progenitor cells in the adult liver [29], we speculated that it might also play a role in embryonic hepatoblast regulation. Alternatively, the liver serves as one of the hematopoietic organs at fetal stages and Hh signaling has been shown to promote embryonic hematopoiesis and vasculogenesis in pre- or early-gastrulation-stage epiblasts [36], raising a possibility that the signal may target blood cells and/or endothelial cells in the fetal liver. To discriminate these possibilities, hepatoblasts were isolated from the fetal liver by auto-MACS using the antibody against Dlk, a well-established surface marker for hepatoblasts [30], and subjected to RT-PCR analyses. The purities of the isolated Dlk^+ and Dlk^- cell fractions were each more than 95% (data not shown). As shown in Fig. 1B, *Gli1* was more strongly induced in Dlk^+ hepatoblasts than in Dlk^- cells, while *Shh* was produced in both cell fractions of the E11.5 and E12.5 livers. These results indicate the transient nature of Hh signal activation during fetal liver development, which primarily targets hepatoblasts at E11.5.

Expression of the ligand *Shh* was observed in E11.5 Dlk^- cells, which is a heterogenous population composed of many types of cells. In order to characterize the Shh-producing cells, we isolated various cell fractions from the E11.5 fetal liver by FACS and analyzed the *Shh* expression (Fig. 1C). We sorted the fetal liver cells

based on the expression of CD45, Ter119, Stab2 and p75NTR, the surface markers for hematopoietic cells, erythroid cells, hepatic sinusoidal endothelial cells [32] and precursors of HSC/portal fibroblasts [31], respectively, in combination with Dlk. As a result, *Shh* was identified to be produced mainly in Dlk^+ hepatoblasts and the $CD45^-/Dlk^-$ fraction, while little or no expression was observed in hepatic sinusoidal endothelial cells, hematopoietic cells or precursors for HSC. The $CD45^-/Dlk^-$ fraction, though not rigorously characterized at the moment, is supposed to contain mesenchymal cells.

To further examine the character of the Hh-responsive cells, we next carried out immunocytochemistry with E11.5 fetal liver cells (Fig. 2). Freshly isolated Dlk^+ hepatoblasts were mostly $Gli1^+$ (Figs. 2A–D; higher magnification images shown in Supplementary Fig. 1) while Dlk^- cells were composed of both $Gli1^+$ and $Gli1^-$ cells (Figs. 2I–L), consistent with the results obtained by the RT-PCR analyses (Fig. 1B). Since Hh signaling is known to enhance cell proliferation in many types of cells and tissues, we also stained the cells with a marker for cell proliferation activity. In both Dlk^+ and Dlk^- fractions, $Ki67^+$ proliferating cells were observed among

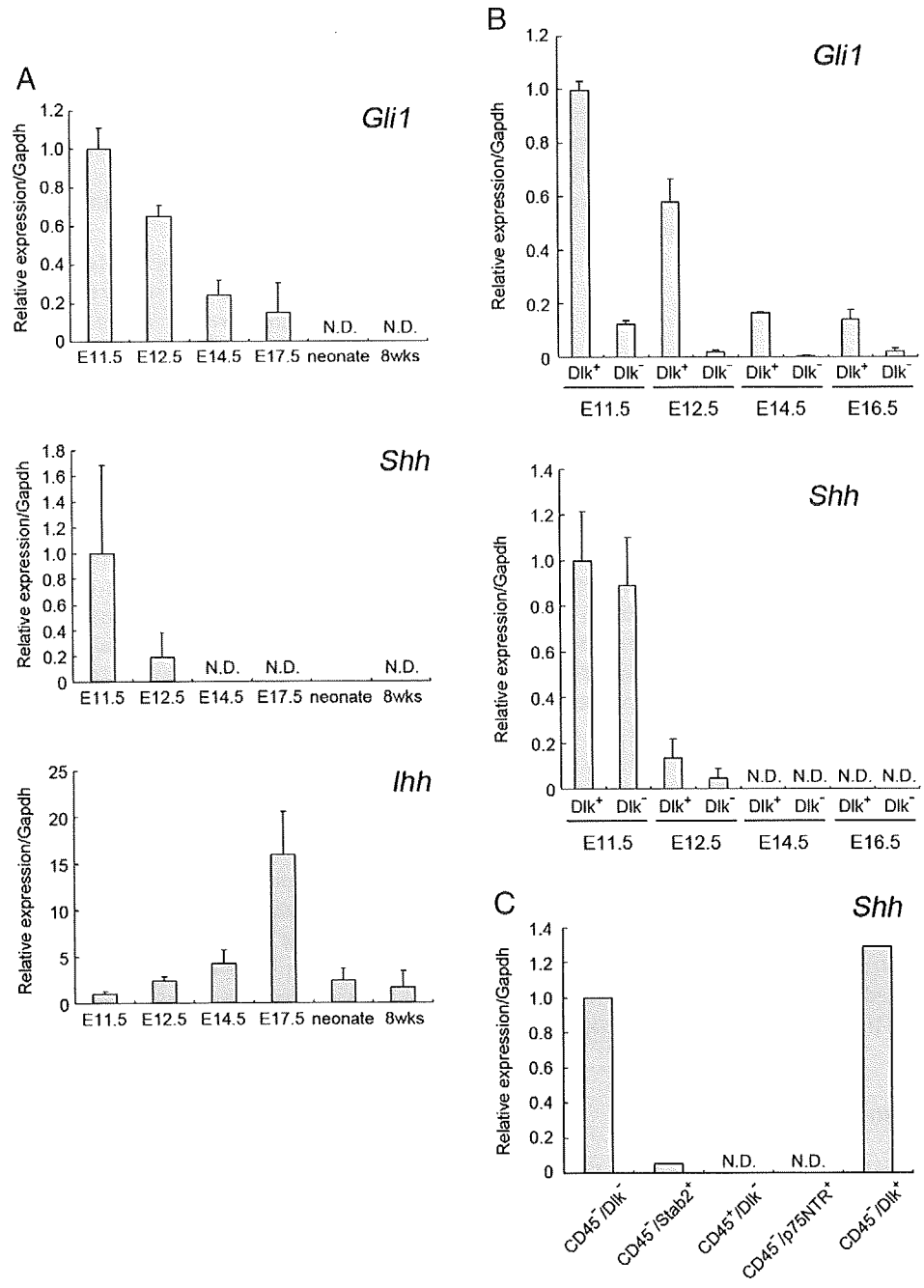

Fig. 1 – Expression of *Gli1*, *Shh* and *Ihh* during the liver development. Relative expression of *Gli1*, *Shh* and *Ihh* in whole liver samples (A; $N=4$), MACS-sorted samples (B; $N=4$) and FACS-sorted samples of the E11.5 fetal liver (C) were analyzed by real-time PCR. Expression levels were normalized using that of *Gapdh*. PI-stained dead cells and $Ter119^+$ erythroid cells were eliminated from all samples in (C). N.D., not detected.

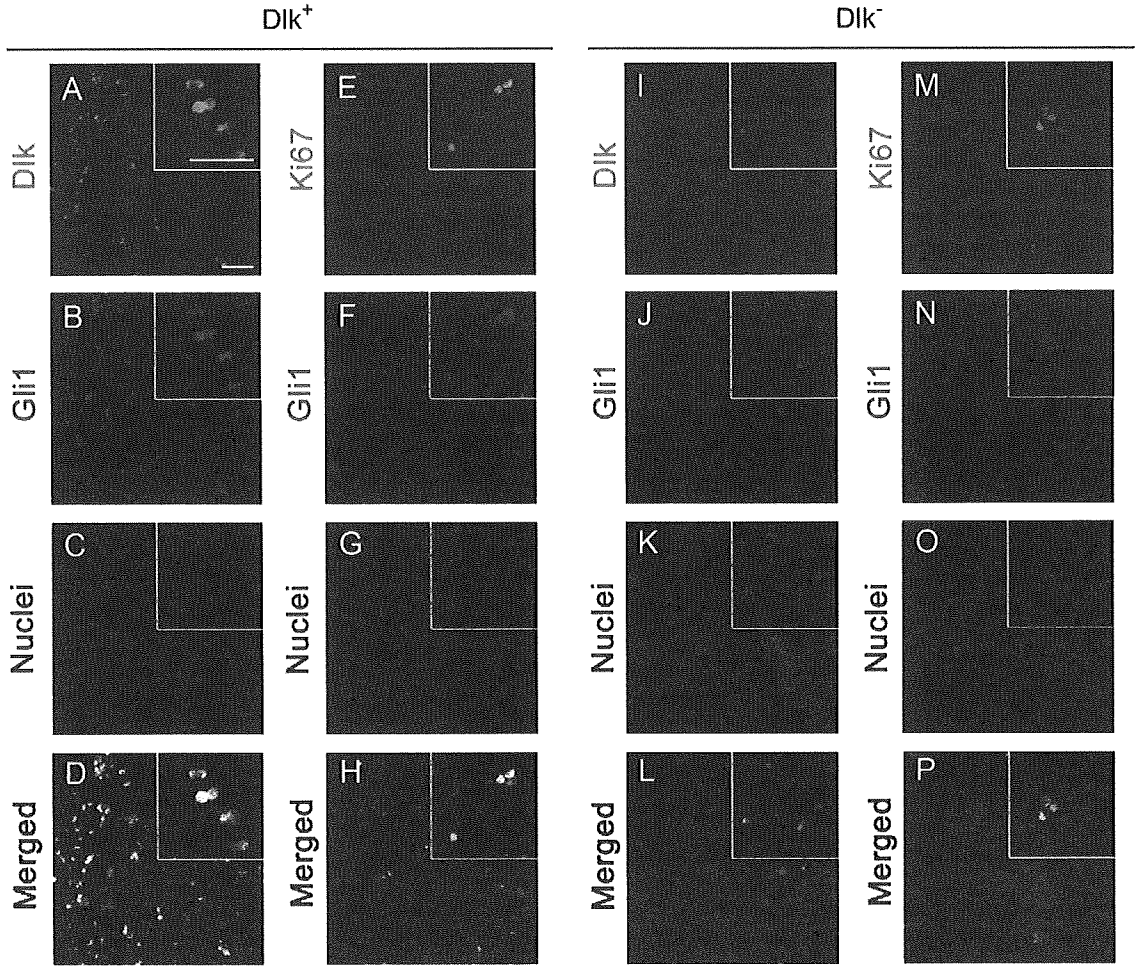

Fig. 2 – Immunocytochemistry of E11.5 Dlk$^+$ and Dlk$^-$ cells. Dlk$^+$ cells (A–H) and Dlk$^-$ cells (I–P) of the E11.5 fetal liver were sorted using MACS and mounted on glass slides by cytospinning. (A–D and I–L) Cells were co-stained with anti-Dlk antibody (A and I; visualized by green) and anti-Gli1 antibody (B and J; visualized by red), together with Hoechst33342 to detect the nuclei (C and K; visualized by blue). Merged images for A–C and I–K are shown in panels D and L, respectively. (E–H and M–P) Cells were co-stained with anti-Ki67 antibody (E and M; visualized by green) and anti-Gli1 antibody (F and N; visualized by red), together with Hoechst33342 to detect the nuclei (G and O; visualized by blue). Merged images for E–G and M–O are shown in panels H and P, respectively. A magnified view is indicated as the inset in each panel. All the panels and insets are each shown at the same magnifications, and the white scale bars in panel A represent 100 μm.

the Gli1$^+$ cells (Figs. 2E–H, M–P). Notably, all the Ki67$^+$ cells were also positive for Gli1. These results suggest a possible relationship between the Hh signal activation and proliferation in fetal liver cells.

Hh signaling stimulates proliferation of hepatoblasts

In order to investigate the direct effect of Hh signal activation on hepatoblast proliferation, we cultured Dlk$^+$ hepatoblasts from the E11.5 fetal liver in the presence of the biologically active form of recombinant Shh (N-terminal fragment of Shh; ShhN). Since Hh signaling was found to be activated at E11.5 but weakened or disappeared at E14.5, we also cultured the hepatoblasts from the latter stage for comparison. In the bulk culture of E11.5 Dlk$^+$ cells, proliferation was significantly promoted by the addition of ShhN in a dose-dependent manner, as well as by a small molecule agonist of Hh signaling, purmorphamine [37] (Fig. 3A and Supplementary Fig. 2). These effects were cancelled in the presence of cyclopamine, a well-established chemical inhibitor of Hh signaling [38]. Proliferation was not affected by cyclopamine alone or EtOH, which was used as the solvent of cyclopamine. On the other hand, neither activation nor inhibition of Hh signaling had any effect on proliferation of E14.5 Dlk$^+$ cells (Fig. 3A). Immunocytochemistry of the cultured E11.5 Dlk$^+$ cells demonstrated that activation of Hh signaling increased the proportion of Ki67$^+$ cells, which were all co-stained with Gli1 (Fig. 3B; higher magnification images shown in Supplementary Fig. 3). This effect was also cancelled by cyclopamine, but not changed by EtOH (data not shown).

To analyze the effect of Hh signaling on the character of hepatoblasts as immature stem/progenitor cells, we next carried out colony formation assays at low cell density, where the cells with stem/progenitor cell activities are considered to be capable of forming relatively large colonies [39]. When Dlk$^+$ cells from the E11.5 fetal liver were cultured under this condition, total cell

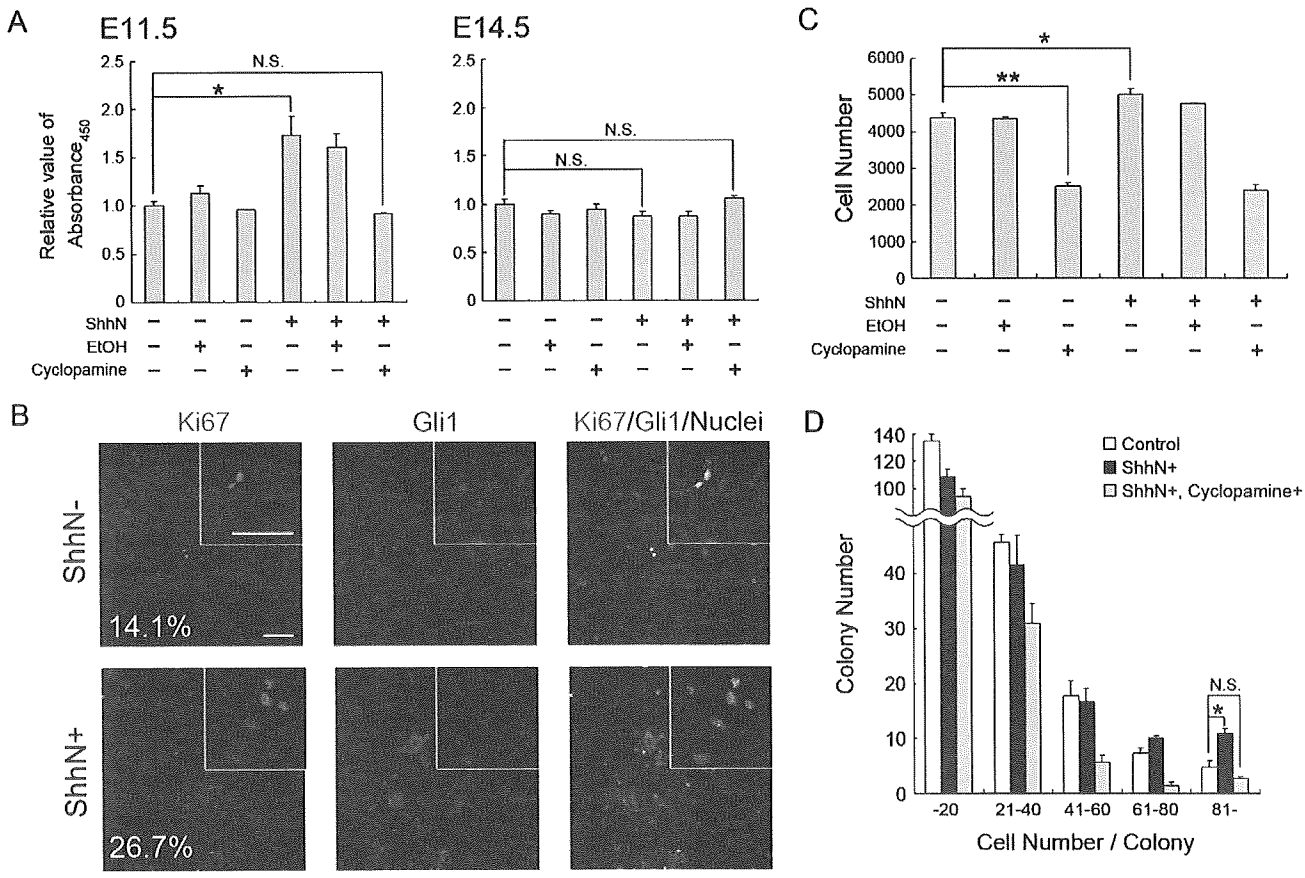

Fig. 3 – Effect of Hh signaling on proliferation of Dlk$^+$ cells. (A) E11.5 and E14.5 Dlk$^+$ cells were cultured for 7 days, and cell proliferation was measured by WST-1 assay. $N=3$. (B) E11.5 Dlk$^+$ cells were cultured for 7 days and stained with anti-Ki67 antibody (green) and anti-Gli1 antibody (red). Merged images are shown in the right column, where nuclear staining by Hoechst33342 is also included (blue). White numbers show percentages of Ki67$^+$ nuclei/total nuclei. White scale bars represent 100 μm. (C) Total cell numbers of the cultured Dlk$^+$ cells after 6 days under the low cell density culture condition. $N=3$. (D) The colony size and frequency in (C) are depicted. The results for the cultures in the absence (control) or presence of ShhN, and with cyclopamine in addition to ShhN are represented. $N=3$. N.S., not significant ($P>0.1$); *$P<0.05$; **$P<0.01$.

numbers were increased by ShhN application while decreased by cyclopamine (Fig. 3C). Intriguingly, the number of the large colonies (defined as those comprising more than 80 cells in this study) was significantly increased by activation of Hh signaling (Fig. 3D). Taken together, these results indicate that Hh signaling can enhance proliferation of hepatoblasts.

Hh signaling has an inhibitory effect on hepatic differentiation of hepatoblasts

We previously demonstrated that differentiation of hepatoblasts into hepatocytes can be faithfully recapitulated in *in vitro* culture of E14.5 Dlk$^+$ cells [30], and have noticed that the same differentiation-inducing protocol can also be applicable to E11.5 Dlk$^+$ cells, as judged by induction of various marker genes for differentiated hepatocytes as well as by several functional assessments (see below, and data not shown). Using this *in vitro* culture system, we aimed to analyze the effect of Hh signaling on hepatocyte differentiation of hepatoblasts. After 10 days of culture, E11.5 Dlk$^+$ cells underwent differentiation into hepatocytes and expressed marker genes for differentiated hepatocytes, *tyrosine aminotransferase* (*Tat*) and *carbamoyl-phosphate synthetase 1* (*Cps1*) (Fig. 4A). Hh signaling activity in the cultured cells as monitored by *Gli1* expression declined after induction of the differentiation, consistently with its transition *in vivo* (Fig. 1A). We then administrated ShhN to these cultures to forcibly activate Hh signaling during the course of differentiation, which resulted in dramatic decrease in the expression of *Tat* and *Cps1* (Fig. 4A). A similar effect of ShhN was also observed in the culture of E14.5 Dlk$^+$ cells (Fig. 4B). Addition of cyclopamine diminished the ectopic Hh signal activation and its inhibitory effect on hepatocyte differentiation. Notably, this resulted in not only restored but rather augmented levels of *Tat* and *Cps1* expression (Fig. 4C). Cyclopamine treatment in the absence of the exogenous ShhN also gave a similar enhancing effect, suggesting that inhibition of the endogenous, autocrine Hh signaling *in vitro* may potentiate hepatic differentiation of hepatoblasts (Fig. 4C).

To further confirm the inhibitory effect of Hh signaling on hepatocyte differentiation, we also tested a metabolic function of the cultured Dlk$^+$ cells. As Cps1 is a key enzyme of the urea cycle and synthesizes carbamoyl phosphate from ammonia [40], we chose to measure ammonia clearance activity of the differentiated

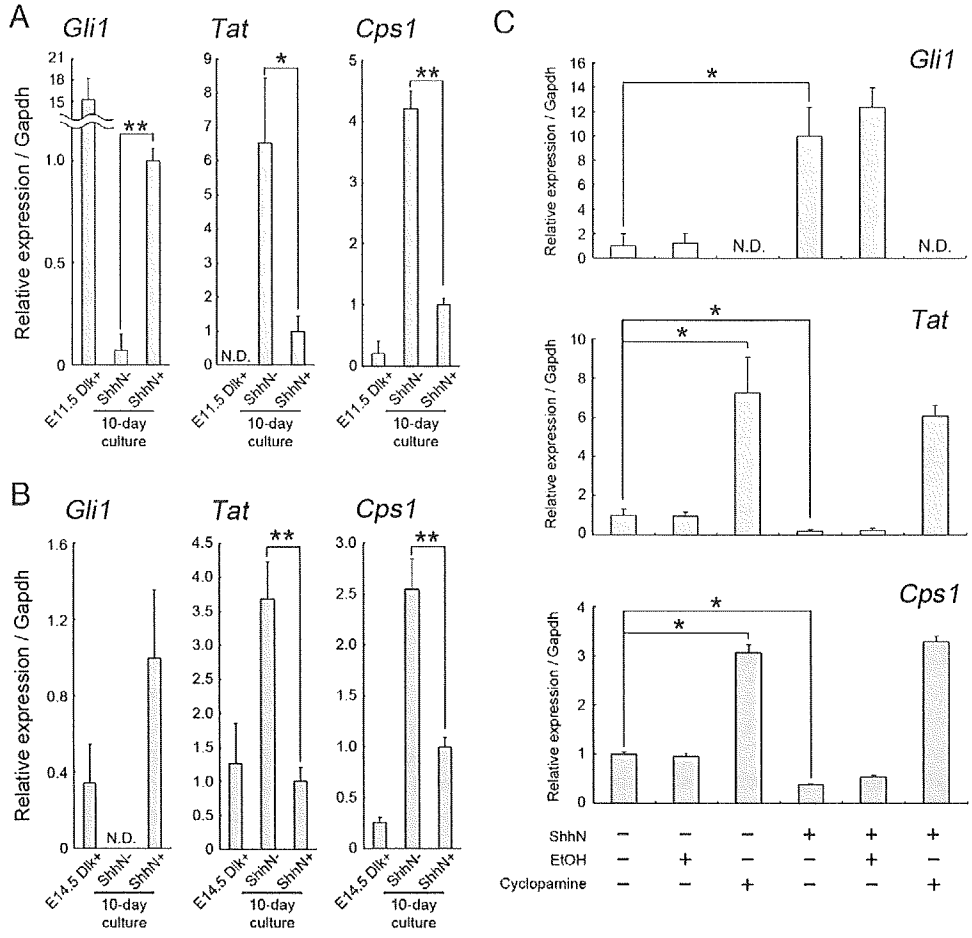

Fig. 4 – Effect of Hh signaling on expression of hepatocyte marker genes. E11.5 Dlk$^+$ cells (A and C) and E14.5 Dlk$^+$ cells (B) were cultured for 10 days, and relative expression of *Gli1*, *Tat* and *Cps1* was measured using real-time RT-PCR. Expression levels were normalized using that of *Gapdh*. $N=4$. N.D. not detected; *$P<0.05$; **$P<0.01$.

hepatocytes. In both E11.5 and E14.5 hepatoblast cultures, ammonia concentration in the medium was declined by the differentiated cells, and the clearance kinetics was delayed in those cells that were differentiated in the presence of ShhN (Fig. 5, and data not shown). This inhibitory effect of ShhN was cancelled by addition of cyclopamine during the differentiation process. In contrast to the case with the marker gene expression, however, cyclopamine treatment did not further enhance the clearance activity beyond the basal level in this assay. Nonetheless, these results together indicate that Hh signaling inhibits functional differentiation to hepatocytes of embryonic hepatoblasts.

Discussion

The progression of organogenesis relies on multiple modes of interaction between tissues and/or cells and thus is tightly and precisely regulated by coordinated actions of various extracellular signals, such as those mediated by cell adhesion molecules, ECMs, as well as growth factors. With respect to the liver development, critical roles of FGF, BMP, Wnt, and several other growth factors or cytokines have already been well appreciated, yet the entire picture of the regulatory signals throughout the whole process still remains to be elucidated. In this study, we have added Shh to the list of those signals, which plays an important role in modulating proliferation and differentiation of hepatoblasts.

By using real-time RT-PCR and immunostaining analyses, we showed that Hh signaling was transiently activated in the fetal liver at E11.5, according to the appearance and proliferation of hepatoblasts (Figs. 1 and 2). Indeed, the signal activation was observed primarily in Dlk$^+$ hepatoblasts, while expression of the corresponding ligand Shh was achieved by both Dlk$^+$ hepatoblasts and Dlk$^-$ cells (Figs. 1B and C). Thus, hepatoblasts at this stage are targeted by Hh signaling in both autocrine and paracrine fashions, similar to the situation observed with adult colon cells [41].

In the E11.5 fetal liver, a weaker yet significant level of *Gli1* expression was also detected in Dlk$^-$ cells, indicating activation and a possible function of Hh signaling therein. Our preliminary experiments employing the FACS-sorted cell fractions suggest that the signal is activated in the p75NTR$^+$ precursors of HSC/portal fibroblast (Y. Hirose, T. Itoh, and A. Miyaima, unpublished observation). In the adult liver, Shh is known to function as an autocrine activation and viability factor for HSC [22,24]. Since *Shh* expression is absent in fetal p75NTR$^+$ cells (Fig. 1C), it is not likely an autocrine but rather a paracrine factor for HSCs in the fetal liver and may play a role in regulating their development, which needs to be addressed in future studies.

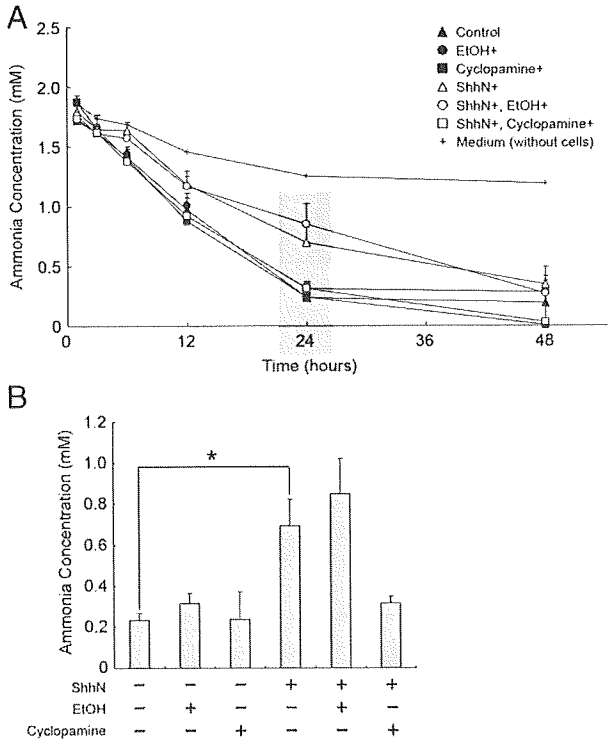

Fig. 5 – Effect of Hh signaling on acquisition of the ammonia clearance ability. After the culture of E11.5 Dlk$^+$ cells for 10 days in the presence or absence of ShhN, cyclopamine, and EtOH (vehicle for cyclopamine), the culture media were replaced with the fresh medium containing 2 mM of NH_3. Ammonia concentration in the media was measured at the indicated time points. The values for ammonia concentration at 24 h were extracted in (B). $N=3$. *$P<0.05$.

In addition to the *Shh* expression at early to mid stages of liver organogenesis, we also observed increasing expression of *Ihh* in the fetal liver, peaking at around the perinatal stage. In the case of this ligand, however, concomitant elevation of *Gli1* expression was not observed (Fig. 1A). Notably, a previous study using C3H10T1/2 cells and some embryonic tissues has reported that the effect of Ihh is weaker than that of Shh [42]. In fact, we also applied the N-terminal fragment of Ihh to the *in vitro* culture of E14.5 Dlk$^+$ hepatoblasts to activate Hh signaling, but the effect was weaker than that of ShhN (data not shown). Interestingly, Ihh has been shown to be expressed in around ductal plates, the precursor for bile ducts, in fetal human livers [29] as well as in bile ductular cells in injured adult livers [20,23]. It is thus of considerable possibility that Ihh signaling may be involved in bile duct formation and, as such, local activation of the downstream signaling in/around those limited structures is not strong enough to be detected in our analysis using the whole liver samples.

By adapting our previously established culture protocol of E14.5 Dlk$^+$ hepatoblasts, where the cells can proliferate and then undergo hepatocyte differentiation with marker gene expression and functional maturation [30,43], we have approached *in vitro* the functional relevance of the Shh expression and signal activation in E11.5 Dlk$^+$ hepatoblasts (Figs. 3–5). In the culture of E11.5 Dlk$^+$ cells, stimulation with ShhN promoted their proliferation (Figs. 3A and B). In accord with this *in vitro* result, some Gli1$^+$ Hh-responsive cells were also positive for Ki67 in the freshly isolated Dlk$^+$ fraction (Figs. 2A–F). Together with the observation in the colony formation assays at lower cell density, where total cell numbers were increased by ShhN stimulation while decreased by cyclopamine (Fig. 3C), our results indicate that Hh signaling activates hepatoblast proliferation in the E11.5 fetal liver. Noticeably, cyclopamine treatment alone (i.e., in the absence of exogenous Shh stimulation) significantly affected proliferation of E11.5 Dlk$^+$ cells in the colony formation assay (Fig. 3C), but failed to do so under the differentiation-inducing culture condition (Fig. 3A). The latter condition is considered to recapitulate, at least in part, the developmental process *in vivo*, where Dlk$^+$ hepatoblasts are prone to lose their *Shh* expression as the differentiation progresses (Figs. 1A and B). Under this condition, the autocrine Hh signaling in hepatoblasts are supposed to be attenuated and hence the inhibitory effect of cyclopamine could not be detected. In contrast, the cells are not actively induced to differentiate in the colony formation assay and are thus considered to better maintain their original character with autocrine Hh signaling, leading to the observed inhibitory effect of cyclopamine on their proliferation.

It should be noted that, in contrast to E11.5 hepatoblasts where ShhN showed a growth-stimulatory effect, in the E14.5 cells neither activation nor inhibition of Hh signaling had any effect on proliferation even though application of ShhN did seem to activate the signaling therein to a considerable extent (Figs. 3A and 4B). Thus, intrinsic cellular program to respond to Hh signal activation is likely to be changed in hepatoblasts during this period of development, although the underlying molecular basis remains to be elucidated. Considering the fact that the ligand expression in the fetal liver rapidly declines during the same period, this may constitute another level of regulatory mechanism that ensures the progression of the hepatoblast development from proliferating to differentiating stages. It is also interesting to note that, during the culture of E11.5 Dlk$^+$ cells under the differentiation-inducing condition, the cells showed a tendency to gradually lose their *Gli1* expression even in the continuous presence of exogenous ShhN, resulting after 10 days of culture in a 15-fold lower level of the expression compared to the initial level when the culture was started (Fig. 4A, and data not shown). As continuous Hh signal activation was found to be deleterious for differentiation of hepatoblasts to hepatocytes, it is tempting to speculate that hepatoblasts may also be programmed so that they lose their ability to receive and/or transduce Hh signaling during the course of differentiation, which may help further establish a robust system to warrant proper development of hepatocytes.

As mentioned above, Ihh expression has been detected in around ductal plates and bile ducts in fetal and adult livers, respectively. The periportal region containing these structures have been considered as putative hepatic stem/progenitor cell compartments, and a previous study has implicated the role of Ihh signal activation there in maintaining resident hepatic stem/progenitor cells [29]. As the formation of ductal plates starts at around E15.5 in mouse embryos [1,44], it remained unclear whether and how Ihh or any other signals were involved in stem/progenitor cell regulation in the fetal liver at earlier stages. In our colony formation assays using E11.5 hepatoblasts, the numbers of relatively large colonies, which are assumed to derive from a more immature stem/progenitor cell population with higher proliferative potentials, were significantly augmented by Hh signal

activation (Fig. 3D). These findings together illuminate the unified activity, as well as the diversified modes of action, of Hh signaling in regulating hepatic stem/progenitor cells. That is, at E11.5 Shh is likely involved in transient expansion of hepatoblasts with their immature phenotype being maintained, while at the later stages Ihh signaling around the ductal structures in turn mediates local maintenance of resident hepatic stem/progenitor cells.

During the course of fetal liver development, Shh expression is initially observed at the very early stage, around E8.5, in the ventral foregut endoderm, and then lost at E9.0–9.5 in the liver bud primordium [25–27]. Based on the results obtained using the *Hex* mutant mice, it is assumed that ectopic expression of *Shh* at the latter stage is deleterious to the proper development of the liver bud, due presumably to its inhibitory activity toward the epithelial morphological transition of the hepatic endodermal cells [28]. Together with these previous findings, our present study has established a hitherto unidentified, highly dynamic feature of the Shh signal activation, as well as its multiple effects on hepatoblast regulation, during the liver organogenesis. Notably, it has been shown that Wnt signaling is initially inhibitory to liver induction at early stages, but rather enhances liver bud growth and differentiation later in development [45]. In a similar way to Wnt signaling, Hh signaling has several distinct and potentially contradictory roles at different stages of embryonic livers, so that expression of the ligand and activation of the signaling pathway need to be strictly regulated for the liver development to proceed normally. It has been reported that the formation of the liver bud occurs in both $Shh^{-/-}$ and $Gli2^{-/-}Gli3^{-/-}$ mouse embryos at E9.5, although the size is smaller than normal in the latter case [46,47]. Future studies using these kinds of *in vivo* models, with a particular focus on the hepatoblast behavior and hepatic differentiation, should pave the way to fully understand the role that Hh signaling plays during the liver organogenesis.

Acknowledgments

We thank Drs. M. Tanaka and N. Tanimizu for valuable suggestions and technical assistance, and the members of the Miyajima laboratory for helpful discussions.

Appendix A. Supplementary data

Supplementary data associated with this article can be found, in the online version, at doi:10.1016/j.yexcr.2009.06.018.

REFERENCES

[1] N. Tanimizu, A. Miyajima, Molecular mechanism of liver development and regeneration, Int. Rev. Cytol. 259 (2007) 1–48.
[2] J.M. Rossi, N.R. Dunn, B.L. Hogan, K.S. Zaret, Distinct mesodermal signals, including BMPs from the septum transversum mesenchyme, are required in combination for hepatogenesis from the endoderm, Genes Dev. 15 (2001) 1998–2009.
[3] K.S. Zaret, Liver specification and early morphogenesis, Mech. Dev. 92 (2000) 83–88.
[4] R. Zhao, S.A. Duncan, Embryonic development of the liver, Hepatology 41 (2005) 956–967.
[5] K. Matsumoto, H. Yoshitomi, J. Rossant, K.S. Zaret, Liver organogenesis promoted by endothelial cells prior to vascular function, Science 294 (2001) 559–563.
[6] C. Schmidt, F. Bladt, S. Goedecke, V. Brinkmann, W. Zschiesche, M. Sharpe, E. Gherardi, C. Birchmeier, Scatter factor/hepatocyte growth factor is essential for liver development, Nature 373 (1995) 699–702.
[7] M. Weinstein, S.P. Monga, Y. Liu, S.G. Brodie, Y. Tang, C. Li, L. Mishra, C.X. Deng, Smad proteins and hepatocyte growth factor control parallel regulatory pathways that converge on beta1-integrin to promote normal liver development, Mol. Cell. Biol. 21 (2001) 5122–5131.
[8] A. Micsenyi, X. Tan, T. Sneddon, J.H. Luo, G.K. Michalopoulos, S.P. Monga, Beta-catenin is temporally regulated during normal liver development, Gastroenterology 126 (2004) 1134–1146.
[9] T. Kinoshita, K. Nagata, N. Sorimachi, H. Karasuyama, T. Sekiguchi, A. Miyajima, Oncostatin M suppresses generation of lymphoid progenitors in fetal liver by inhibiting the hepatic microenvironment, Exp. Hematol. 29 (2001) 1091–1097.
[10] A. Kamiya, T. Kinoshita, Y. Ito, T. Matsui, Y. Morikawa, E. Senba, K. Nakashima, T. Taga, K. Yoshida, T. Kishimoto, A. Miyajima, Fetal liver development requires a paracrine action of oncostatin M through the gp130 signal transducer, EMBO J. 18 (1999) 2127–2136.
[11] A. Kamiya, T. Kinoshita, A. Miyajima, Oncostatin M and hepatocyte growth factor induce hepatic maturation via distinct signaling pathways, FEBS Lett. 492 (2001) 90–94.
[12] A. Kamiya, N. Kojima, T. Kinoshita, Y. Sakai, A. Miyaijma, Maturation of fetal hepatocytes *in vitro* by extracellular matrices and oncostatin M: induction of tryptophan oxygenase, Hepatology 35 (2002) 1351–1359.
[13] M. Varjosalo, J. Taipale, Hedgehog: functions and mechanisms, Genes Dev. 22 (2008) 2454–2472.
[14] S. Roy, P.W. Ingham, Hedgehogs tryst with the cell cycle, J. Cell. Sci. 115 (2002) 4393–4397.
[15] J.E. Hooper, M.P. Scott, Communicating with Hedgehogs, Nat. Rev., Mol. Cell. Biol. 6 (2005) 306–317.
[16] J. Jiang, C.C. Hui, Hedgehog signaling in development and cancer, Dev. Cell 15 (2008) 801–812.
[17] P.A. Beachy, S.S. Karhadkar, D.M. Berman, Tissue repair and stem cell renewal in carcinogenesis, Nature 432 (2004) 324–331.
[18] A.P. McMahon, P.W. Ingham, C.J. Tabin, Developmental roles and clinical significance of hedgehog signaling, Curr. Top. Dev. Biol. 53 (2003) 1–114.
[19] S. Huang, J. He, X. Zhang, Y. Bian, L. Yang, G. Xie, K. Zhang, W. Tang, A.A. Stelter, Q. Wang, H. Zhang, J. Xie, Activation of the hedgehog pathway in human hepatocellular carcinomas, Carcinogenesis 27 (2006) 1334–1340.
[20] Y. Jung, S.J. McCall, Y.X. Li, A.M. Diehl, Bile ductules and stromal cells express hedgehog ligands and/or hedgehog target genes in primary biliary cirrhosis, Hepatology 45 (2007) 1091–1096.
[21] M. Eichenmuller, I. Gruner, B. Hagl, B. Haberle, J. Muller-Hocker, D. von Schweinitz, R. Kappler, Blocking the hedgehog pathway inhibits hepatoblastoma growth, Hepatology 49 (2008) 482–490.
[22] L. Yang, Y. Wang, H. Mao, S. Fleig, A. Omenetti, K.D. Brown, J.K. Sicklick, Y.X. Li, A.M. Diehl, Sonic hedgehog is an autocrine viability factor for myofibroblastic hepatic stellate cells, J. Hepatol. 48 (2008) 98–106.
[23] A. Omenetti, L. Yang, Y.X. Li, S.J. McCall, Y. Jung, J.K. Sicklick, J. Huang, S. Choi, A. Suzuki, A.M. Diehl, Hedgehog-mediated mesenchymal–epithelial interactions modulate hepatic response to bile duct ligation, Lab. Invest. 87 (2007) 499–514.
[24] J.K. Sicklick, Y.X. Li, S.S. Choi, Y. Qi, W. Chen, M. Bustamante, J. Huang, M. Zdanowicz, T. Camp, M.S. Torbenson, M. Rojkind, A.M. Diehl, Role for hedgehog signaling in hepatic stellate cell activation and viability, Lab. Invest. 85 (2005) 1368–1380.
[25] Y. Echelard, D.J. Epstein, B. St-Jacques, L. Shen, J. Mohler, J.A. McMahon, A.P. McMahon, Sonic hedgehog, a member of a family of putative signaling molecules, is implicated in the regulation of CNS polarity, Cell 75 (1993) 1417–1430.

[26] L.V. Goodrich, R.L. Johnson, L. Milenkovic, J.A. McMahon, M.P. Scott, Conservation of the hedgehog/patched signaling pathway from flies to mice: induction of a mouse patched gene by Hedgehog, Genes Dev. 10 (1996) 301–312.
[27] Z. Burke, G. Oliver, Prox1 is an early specific marker for the developing liver and pancreas in the mammalian foregut endoderm, Mech. Dev. 118 (2002) 147–155.
[28] R. Bort, M. Signore, K. Tremblay, J.P. Martinez Barbera, K.S. Zaret, Hex homeobox gene controls the transition of the endoderm to a pseudostratified, cell emergent epithelium for liver bud development, Dev. Biol. 290 (2006) 44–56.
[29] J.K. Sicklick, Y.X. Li, A. Melhem, E. Schmelzer, M. Zdanowicz, J. Huang, M. Caballero, J.H. Fair, J.W. Ludlow, R.E. McClelland, L.M. Reid, A.M. Diehl, Hedgehog signaling maintains resident hepatic progenitors throughout life, Am. J. Physiol.: Gasterointest. Liver Physiol. 290 (2006) G859–870.
[30] N. Tanimizu, M. Nishikawa, H. Saito, T. Tsujimura, A. Miyajima, Isolation of hepatoblasts based on the expression of Dlk/Pref-1, J. Cell. Sci. 116 (2003) 1775–1786.
[31] K. Suzuki, M. Tanaka, N. Watanabe, S. Saito, H. Nonaka, A. Miyajima, p75 Neurotrophin receptor is a marker for precursors of stellate cells and portal fibroblasts in mouse fetal liver, Gastroenterology 135 (2008) 270–281 e273.
[32] H. Nonaka, M. Tanaka, K. Suzuki, A. Miyajima, Development of murine hepatic sinusoidal endothelial cells characterized by the expression of hyaluronan receptors, Dev. Dyn. 236 (2007) 2258–2267.
[33] N. Kojima, T. Kinoshita, A. Kamiya, K. Nakamura, K. Nakashima, T. Taga, A. Miyajima, Cell density-dependent regulation of hepatic development by a gp130-independent pathway, Biochem. Biophys. Res. Commun. 277 (2000) 152–158.
[34] M.J. Bitgood, L. Shen, A.P. McMahon, Sertoli cell signaling by Desert hedgehog regulates the male germline, Curr. Biol. 6 (1996) 298–304.
[35] E. Parmantier, B. Lynn, D. Lawson, M. Turmaine, S.S. Namini, L. Chakrabarti, A.P. McMahon, K.R. Jessen, R. Mirsky, Schwann cell-derived Desert hedgehog controls the development of peripheral nerve sheaths, Neuron 23 (1999) 713–724.
[36] M.A. Dyer, S.M. Farrington, D. Mohn, J.R. Munday, M.H. Baron, Indian hedgehog activates hematopoiesis and vasculogenesis and can respecify prospective neurectodermal cell fate in the mouse embryo, Development 128 (2001) 1717–1730.
[37] X. Wu, J. Walker, J. Zhang, S. Ding, P.G. Schultz, Purmorphamine induces osteogenesis by activation of the hedgehog signaling pathway, Chem. Biol. 11 (2004) 1229–1238.
[38] J.P. Incardona, W. Gaffield, R.P. Kapur, H. Roelink, The teratogenic Veratrum alkaloid cyclopamine inhibits sonic hedgehog signal transduction, Development 125 (1998) 3553–3562.
[39] A. Suzuki, Y.W. Zheng, S. Kaneko, M. Onodera, K. Fukao, H. Nakauchi, H. Taniguchi, Clonal identification and characterization of self-renewing pluripotent stem cells in the developing liver, J. Cell Biol. 156 (2002) 173–184.
[40] H.M. Holden, J.B. Thoden, F.M. Raushel, Carbamoyl phosphate synthetase: an amazing biochemical odyssey from substrate to product, Cell. Mol. Life Sci. 56 (1999) 507–522.
[41] G.R. van den Brink, Hedgehog signaling in development and homeostasis of the gastrointestinal tract, Physiol. Rev. 87 (2007) 1343–1375.
[42] S. Pathi, S. Pagan-Westphal, D.P. Baker, E.A. Garber, P. Rayhorn, D. Bumcrot, C.J. Tabin, R. Blake Pepinsky, K.P. Williams, Comparative biological responses to human Sonic, Indian, and Desert hedgehog, Mech. Dev. 106 (2001) 107–117.
[43] N. Tanimizu, H. Saito, K. Mostov, A. Miyajima, Long-term culture of hepatic progenitors derived from mouse Dlk^{+} hepatoblasts, J. Cell. Sci. 117 (2004) 6425–6434.
[44] F.P. Lemaigre, Development of the biliary tract, Mech. Dev. 120 (2003) 81–87.
[45] V.A. McLin, S.A. Rankin, A.M. Zorn, Repression of Wnt/beta-catenin signaling in the anterior endoderm is essential for liver and pancreas development, Development 134 (2007) 2207–2217.
[46] Y. Litingtung, L. Lei, H. Westphal, C. Chiang, Sonic hedgehog is essential to foregut development, Nat. Genet. 20 (1998) 58–61.
[47] J. Motoyama, J. Liu, R. Mo, Q. Ding, M. Post, C.C. Hui, Essential function of Gli2 and Gli3 in the formation of lung, trachea and oesophagus, Nat. Genet. 20 (1998) 54–57.

Development 137, 159-167 (2010) doi:10.1242/dev.041574

A novel regulatory mechanism for Fgf18 signaling involving cysteine-rich FGF receptor (Cfr) and delta-like protein (Dlk)

Yuichiro Miyaoka[1], Minoru Tanaka[2], Toru Imamura[3], Shinji Takada[4,5] and Atsushi Miyajima[1,*]

SUMMARY

Fibroblast growth factors (FGFs) transduce signals through FGF receptors (FGFRs) and have pleiotropic functions. Besides signal-transducing FGFRs, cysteine-rich FGF receptor (Cfr; Glg1) is also known to bind some FGFs, although its physiological functions remain unknown. In this study, we generated *Cfr*-deficient mice and found that some of them die perinatally, and show growth retardation, tail malformation and cleft palate. These phenotypes are strikingly similar to those of *Fgf18*-deficient mice, and we revealed interaction between Cfr and Fgf18 both genetically and physically, suggesting functional cooperation. Consistently, introduction of Cfr facilitated Fgf18-dependent proliferation of Ba/F3 cells expressing Fgfr3c. In addition, we uncovered binding between Cfr and delta-like protein (Dlk), and noticed that *Cfr*-deficient mice are also similar to *Dlk*-transgenic mice, indicating that Cfr and Dlk function in opposite ways. Interestingly, we also found that Dlk interrupts the binding between Cfr and Fgf18. Thus, the Fgf18 signaling pathway seems to be finely tuned by Cfr and Dlk for skeletal development. This study reveals a novel regulatory mechanism for Fgf18 signaling involving Cfr and Dlk.

KEY WORDS: Cysteine-rich FGF receptor (Cfr), Delta-like protein (Dlk), Fibroblast growth factor 18 (Fgf18)

INTRODUCTION

The fibroblast growth factor (FGF) family consists of 22 members in mice and humans, and has pleiotropic roles. Gene targeting studies have clearly demonstrated that some FGFs are indispensable to the development of many organs and tissues, including the limbs, lungs, liver, brain, testes, hair follicles and skeleton (Eswarakumar et al., 2005). FGFs transduce intracellular signals via FGF receptors (FGFRs) with a tyrosine kinase. As there are four genes encoding FGFRs in mice and humans, and Fgfr1, Fgfr2 and Fgfr3 each have two splice variants, the FGFR family consists of seven members. Each FGFR binds a subset of FGFs and transduces signals by forming an active receptor complex (Eswarakumar et al., 2005). Besides FGFRs, there are several FGF-binding molecules that also contribute to FGF signaling. Heparan sulfate proteoglycans (HSPGs) are necessary for the dimerization and activation of FGFRs by FGFs (Spivak-Kroizman et al., 1994; Yayon et al., 1991). Klothos are transmembrane proteins that modify the specificity of FGFRs by forming complexes with them and are indispensable for signaling by the FGFs with endocrine functions: i.e. Fgf19 (Fgf15 – Mouse Genome Informatics), Fgf21 and Fgf23 (Kurosu et al., 2007; Kurosu et al., 2006; Suzuki et al., 2008b; Urakawa et al., 2006). FGFR-like 1 (Fgfrl1), which shares sequence homology with FGFRs in its extracellular domain, but lacks an intracellular tyrosine-kinase, is also involved in FGF signaling (Wiedemann and Trueb, 2000). FGFRL1 seems to be a decoy receptor that negatively regulates FGF signaling (Trueb et al., 2003), and has indispensable roles in the development of the diaphragm (Baertschi et al., 2007). Thus, the modulation of FGF signaling by FGF-binding molecules plays important roles in normal developmental processes.

Cysteine-rich FGF receptor (Cfr; Glg1 – Mouse Genome Informatics) is another non-FGFR FGF-binding molecule, which was identified as a transmembrane molecule with affinity for Fgf1 and Fgf2 (Burrus and Olwin, 1989), and subsequently shown to bind Fgf3 and Fgf4 (Burrus et al., 1992; Kohl et al., 2000). Although Cfr binds FGFs via its large extracellular domain consisting of 16 repeats of an unique motif known as the Cfr repeat, it has no sequence homology with FGFRs and its intracellular domain consists of a short peptide of 13 amino acids without a kinase (Zhou et al., 1997). Thus, Cfr is a unique FGF-binding protein and may play a role in FGF signaling like the other FGF-binding proteins described above; however, its functions remain to be elucidated.

In this study, we identified Cfr as a delta-like protein (Dlk)-binding molecule. Dlk, also known as preadipocyte factor 1 (Pref-1), is a transmembrane protein with six epidermal growth factor (EGF) repeats in its extracellular domain. Dlk has sequence homology with Delta, a ligand for Notch, but lacks the Delta/Serrate/LAG-2 (DSL)-motif required for the activation of Notch. Dlk is abundantly expressed in various embryonic tissues (Smas and Sul, 1993) and we previously identified Dlk as a cell surface marker for hepatoblasts, embryonic hepatic progenitor cells (Tanimizu et al., 2003). *Dlk*-deficient mice show several developmental abnormalities such as perinatal death, growth retardation, skeletal abnormalities, increased amounts of adipose tissue and abnormal B cell development (Moon et al., 2002; Raghunandan et al., 2008), indicating that Dlk plays a fundamental role in development. Having identified Cfr as a Dlk-binding protein, we were interested in the functions of Cfr and the relation between Cfr and Dlk. To reveal the functions of Cfr, we generated *Cfr*-deficient mice and found that some of them die shortly after birth and show growth retardation, tail distortion and cleft palate. Among all the *Fgf*-deficient mice published, *Fgf18*-deficient mice were most similar to *Cfr*-deficient mice in terms of these

[1]Laboratory of Cell Growth and Differentiation, Institute of Molecular and Cellular Biosciences and [2]Promotion of Independence for Young Investigators, The University of Tokyo, Yayoi, Bunkyo-ku, Tokyo 113-0032, Japan. [3]Signaling Molecules Research Laboratory, National Institute of Advanced Industrial Science and Technology (AIST), Tsukuba, Ibaraki 305-8566, Japan. [4]Okazaki Institute for Integrative Biosciences, National Institutes of Natural Sciences, and [5]Department of Basic Biology, Graduate University for Advanced Studies (SOKENDAI), Okazaki, Aichi 444-8787, Japan.

*Author for correspondence (miyajima@iam.u-tokyo.ac.jp)

Accepted 21 October 2009

phenotypes (Liu et al., 2002; Ohbayashi et al., 2002). Fgf18 activates intracellular signaling mainly via Fgfr3c (Zhang et al., 2006), and it is well established that Fgf18-Fgfr3c signaling plays a central role in skeletal development (Haque et al., 2007). Fgf18 inhibits the proliferation of chondrocytes (Liu et al., 2002; Ohbayashi et al., 2002), and several Fgfr3 mutations in humans are known to be a cause of dwarfism (Horton et al., 2007). In this paper, we show genetic and physical interaction between Cfr and Fgf18, and a positive regulatory role of Cfr in Fgf18 signaling. Moreover, we also noticed that the phenotypes of *Cfr*-deficient mice are similar to those of *Dlk*-transgenic mice (Lee et al., 2003) and found that Dlk inhibits the physical interaction between Cfr and Fgf18. Taken together, these results imply that Dlk interferes with the positive regulatory role of Cfr in Fgf18 signaling by abrogating the binding between Cfr and Fgf18. Thus, our study reveals a novel regulatory mechanism for Fgf18 signaling involving Cfr and Dlk.

MATERIALS AND METHODS

Mice

Cfr-deficient mice were generated by using a gene-trapped 129Ola embryonic stem (ES) cell line (see Results). The cell line used for this research project, BayGenomics clone KST005 (catalog number 000716-UCD), was obtained from the Mutant Mouse Regional Resource Center (MMRRC), a NCRR-NIH funded strain repository, and was donated to the MMRRC by the NIH and NHLBI supported BayGenomics consortium. The mouse model will be made available (BRC No. RBRC03897) from the RIKEN BioResource Center (RIKEN BRC), which is participating in the National Bio-Resource Project of the MEXT, Japan, please contact them at animal@brc.riken.jp for inquiries, or search the catalog at http://www.brc.riken.go.jp/lab/animal/en/. The details of *Fgf18* targeting were described previously (Ohbayashi et al., 2002). The *Cfr*-mutant and *Fgf18*-mutant mice used in this study had been back crossed with C57BL/6 wild-type mice at least eight and ten times, respectively. All experimental procedures in this study were approved by the institutional animal care and use committee of the University of Tokyo.

Antibodies

The antibodies used were as follows: anti-Actin (sc-1616) purchased from Santa Cruz Biotechnology, rat monoclonal antibody against Dlk raised in our laboratory (Suzuki et al., 2008a); anti-Cfr rabbit serum raised against the N-terminal domain of Cfr without a signal sequence (28-256 amino acid residues), which was expressed in *Escherichia coli*, and anti-Fgf18 rabbit serum raised against full-length Fgf18 without a signal sequence, which was fused to a GST tag and expressed in *E. coli*.

Expression screening for Dlk-binding proteins

The extracellular domain of Dlk (1-303 amino acid residues) fused to the human IgG Fc region (Dlk-Fc) was expressed in COS7 cells and purified from the culture supernatant with a Hi Trap column (GE Healthcare), and then biotinylated with a biotinylation module (GE Healthcare) for flow cytometric analysis. First, we constructed a cDNA library of HPPL with the FastTrack 2.0 mRNA Isolation Kit (Invitrogen) and SuperScript Choice System (Invitrogen) in the pMXs retroviral vector. The plasmid was then converted to retrovirus using PLAT-E cells. Ba/F3 cells were infected with the virus library and Ba/F3 cells that bound Dlk-Fc were enriched by IMag (Becton-Dickinson) cell sorting using biotinylated Dlk-Fc protein. Genomic PCR of the sorted cells revealed that some of them had the full-length *Cfr* sequence in their genomes (see Results).

Retroviral gene transfer and proliferation assay of Ba/F3 cells

We utilized a Ba/F3 cell line, which expresses a fusion protein of the extracellular domain of Fgfr3c and the intracellular domain of Fgfr1 described previously (Ornitz et al., 1996). For simplicity, we refer to this fusion protein as Fgfr3c in this report.

We constructed a pMXs-IRES-GFP vector encoding the full-length Cfr and produced retroviruses from the vector using PLAT-E cells as described previously (Miyaoka et al., 2006). Ba/F3 cells were infected with the viruses and cells expressing GFP were sorted by FACSVantage (Becton Dickinson).

For proliferation assay, Ba/F3 cells were deprived of cytokines for at least 6 hours, and then 2×10^3 Ba/F3 cells were cultured in 100 μl RPMI-1640 (SIGMA) containing 10% fetal bovine serum (EQUITECH-BIO), 2 mM L-glutamine, 50 μg/ml gentamicin (Wako), and the indicated reagents per 96 well for 2 or 3 days. We assessed the extent of proliferation by adding 10 μl WST-1 reagent (Roche) per 96 well, incubating at 37°C for 2 hours, and monitoring absorbance at 450 nm subtracted by basal absorbance at 650 nm. We set eight wells per one condition in all the experiments in this report.

Quantitative PCR analysis

For cDNA synthesis, total RNA was isolated with TRIzol Reagent (Invitrogen), and then reverse transcribed with a High Capacity cDNA Reverse Transcription Kit (Applied Biosystems). For analysis, SYBR Premix Ex Taq (Takara) and Light Cycler (Roche) were used.

Histochemistry

For immunohistochemistry, embryos were dissected and fixed with methanol/DMSO (4:1) at 4°C overnight, and then incubated in methanol/DMSO/H_2O_2 (4:1:1) at room temperature for 8 hours. Embryos were rehydrated and incubated with primary antibodies at 4°C overnight. They were then incubated with anti-rat IgG-HRP at 4°C overnight. Signal was visualized with 0.06% DAB/0.06% $NiCl_2$ in PBS with 0.2% BSA, 0.5% Triton X-100 and 0.03% H_2O_2.

For immunofluorescent staining, embryos were dissected and fixed with Zamboni's fixative at 4°C overnight, and then gradually substituted to 20% sucrose in PBS. The samples were sectioned and incubated with 5% skimmed milk in PBS for 2 hours at room temperature. They were then incubated with first antibodies at 4°C overnight, and with second antibody conjugated with Alexa Fluor 488 or 555 (Invitrogen) for 2 hours at room temperature. The sections were embedded with Gel/Mount (Cosmo Bio) containing Hoechst 33342.

For examining β-gal activity, embryos were dissected and fixed with 4% paraformaldehyde in PBS at room temperature for 10 minutes. After being washed with PBS, they were incubated in 1 mg/ml X-Gal, 5 mM ferricyanide, 5 mM ferrocyanide, 2 mM $MgCl_2$, 0.02% Nonidet-P 40 and 40 mM HEPES in PBS at 37°C for appropriate periods.

Western blot analysis and northern blot analysis

The detailed methods for western blot analysis and northern blot analysis were described previously (Miyaoka et al., 2006).

Alcian Blue/Alizarin Red staining of cartilage and bone

Mice were dissected, eviscerated, and fixed with 95% ethanol overnight. They were then incubated in acetone overnight. After a brief rinse with water, the samples were incubated in 20% acetate, 75% ethanol and 0.15 mg/ml Alcian Blue 8GX overnight. Then, the samples were washed with 70% ethanol for 8 hours, and cleared with 1% KOH overnight. For counterstaining, 0.05 mg/ml Alizarin Red in 1% KOH was used, and the samples were cleared in 1% KOH in 20% glycerol. All steps were done at room temperature.

Immunoprecipitation

The extracellular domain of Cfr (1-869 amino acid residues) fused tandemly to a His tag and a FLAG tag at its C-terminus (Cfr-EC) was expressed in COS7 cells and purified by using His Trap column (GE Healthcare). Protein G Sepharose (GE Healthcare) was used for precipitation of Fc-fused proteins. Cfr-EC was immunoprecipitated with anti-Cfr serum and protein G Sepharose, or anti-FLAG M2 agarose (SIGMA). These beads were incubated with culture supernatants or the lysis buffer (Miyaoka et al., 2006) containing their target proteins at 4°C for 4 hours, and then washed with the lysis buffer four times.

RESULTS

Identification of Cfr as a Dlk-binding molecule

First, we attempted to identify molecules that bind to Dlk by using an expression screening method. To find cells expressing Dlk-binding proteins on their surface, the extracelluar domain of Dlk

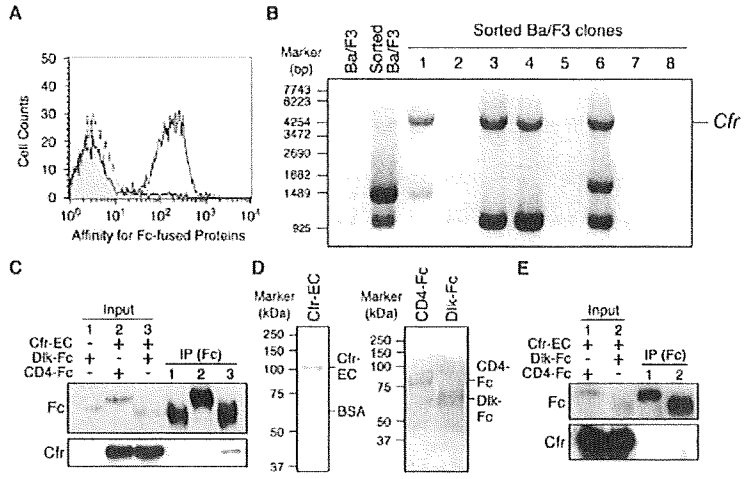

Fig. 1. Identification of Cfr as a Dlk-binding molecule. **(A)** Flow cytometric analysis of the binding of Dlk-Fc protein to HPPL. The specificity of the binding was confirmed with control CD4-Fc protein. Grey, no protein added; dotted line, CD4-Fc; unbroken line, Dlk-Fc. **(B)** DNA fragments inserted by retroviruses in Ba/F3 clones isolated by the cell sorting. Virus-sequence-specific primers amplified the inserted DNA fragments by PCR. Ba/F3, untreated Ba/F3 cells; sorted Ba/F3 cells, the sorted bulk Ba/F3 cells before cloning. **(C)** Immunoprecipitation confirming the binding between Dlk and Cfr. Plasmid constructs shown were introduced into COS7 cells, and Dlk-Fc or CD4-Fc was immunoprecipitated from the culture supernatants. Western blot analysis revealed that the extracellular domain of Cfr (Cfr-EC) was specifically co-immunoprecipitated with Dlk-Fc. **(D)** Coomassie Brilliant Blue staining of Cfr-EC, CD4-Fc and Dlk-Fc purified from COS7 culture supernatants. A weak signal of residual BSA was observed together with that of Cfr-EC. **(E)** Western blot analysis of the immunoprecipitates confirming the binding between the purified Dlk-Fc and Cfr-EC.

was fused to the Fc domain of human IgG (Dlk-Fc) and flow cytometry was used to find cells that bound Dlk-Fc. We found that Dlk-Fc strongly bound to HPPL, a hepatocyte progenitor cell line (Tanimizu et al., 2004) (Fig. 1A). To clone a cDNA encoding the Dlk-binding protein, a retroviral cDNA expression library was constructed from HPPL and introduced into Ba/F3 cells. Magnetic cell sorting was used to enrich Ba/F3 cells that bound Dlk-Fc. After three rounds of enrichment, we obtained several Ba/F3 clones that bound Dlk-Fc. Oligonucleotide primers specific for the retrovirus sequence were used to amplify the sequences introduced into the Ba/F3 genomes by the retrovirus. Sequencing of the amplified DNA fragments revealed that four of the eight clones contained in their genomes a full-length *Cfr* cDNA sequence (Fig. 1B). Other amplified DNA fragments seemed to be non-specific, because they were all truncated, not full-length fragments, and some of them were inserted in the reverse orientation to the retrovirus promoter (data not shown). As clones 1, 3 and 4, and 6 in Fig. 1B had different non-specific fragments inserted in the genomes, these clones were independently generated and acquired the affinity for Dlk-Fc by the *Cfr* insertion. We confirmed binding between Cfr and Dlk by immunoprecipitation. The extracellular domain of Cfr (Cfr-EC) was expressed in COS7 cells together with either Dlk-Fc or the extracellular domain of CD4 fused to the Fc domain of human IgG (CD4-Fc), and the Fc-fusion proteins were immunoprecipitated from the culture supernatants. As shown in Fig. 1C, Cfr-EC was co-precipitated with Dlk-Fc but not CD4-Fc. Then, we purified Cfr-EC, Dlk-Fc and CD4-Fc, and found that the purified Cfr-EC was also co-precipitated with the purified Dlk-Fc (Fig. 1D,E). These results indicate that Cfr directly interacts with Dlk. However, as the signal of the co-precipitated purified Cfr was relatively weak compared with that from the crude culture supernatants (Fig. 1C,E), it might be possible that the interaction is enhanced by other factors.

Generation of *Cfr*-deficient mice

As there has been no report on the physiological role of Cfr, we generated *Cfr*-deficient mice by utilizing a gene-trapped ES cell line. Because this ES cell line has a *β-geo* cassette with a splice acceptor inserted in the first intron of the *Cfr* locus, normal splicing between the first and second exons was interrupted, resulting in the production of a protein in which the peptide from the first exon is fused with β-geo (Fig. 2A). The ES cells were introduced into C57BL/6 blastocysts to generate chimeric mice, and a mouse with ES-cell-derived cells in its germline was obtained. First, we confirmed the site of the *β-geo* cassette in the first intron of the *Cfr* locus by inverse PCR (data not shown), and located it, in the correct orientation, about 10 kbp 3′ downstream from the end of the first exon (Fig. 2A). The insertion was further confirmed to be correct by PCR with primers indicated in Fig. 2A (Fig. 2B). To confirm the abrogation of Cfr protein expression, lysates from embryonic day 11.5 (E11.5) whole embryos of each genotype were subjected to a western blot analysis with antiserum raised against the N-terminal domain of Cfr. An embryo homozygous for the gene-trapped allele showed a protein larger than the wild-type Cfr, the molecular weight of which corresponds to that of a fusion protein comprising the peptide from the first exon of *Cfr* and β-geo. Both the intact Cfr and the fusion protein were detected in a heterozygous embryo (Fig. 2B). Because no intact Cfr protein was detected in the embryo homozygous for the gene-trapped allele, and the first exon of *Cfr* contains only its signal peptide with a few additional amino acid residues (117 amino acid residues), it is highly likely that the gene-trap results in a null mutation. Therefore, we refer to the gene-trapped allele as '-' hereafter. Mating between $Cfr^{+/-}$ mice resulted in the generation of embryos with the normal Mendelian segregation pattern until E18.5; however, about 90% of $Cfr^{-/-}$ mice died within 2 days after birth and there were only a few $Cfr^{-/-}$ mice alive at 3